

High-frequency Miocene sequence stratigraphy, offshore Louisiana: Cycle framework and influence on production distribution in a mature shelf province

Tucker F. Hentz and Hongliu Zeng

ABSTRACT

The regressive Miocene succession of offshore Louisiana comprises 10 third-order sequences and no fewer than 58 fourth-order sequences, which average approximately 1.1 and 0.19 m.y. in duration, respectively, comparable to durations measured in the Gulf Coast Basin and basins worldwide. Upper lower to middle Miocene distal third-order sequences comprise mostly lowstand prograding-wedge, slope-fan, and basin-floor-fan deposits. In contrast, middle to upper Miocene medial sequences record progressively more landward systems tracts: (1) the lateral transition between on-shelf incised-valley fills and the proximal parts of basinward-thickening, lowstand prograding wedges and (2) cyclic on-shelf highstand and transgressive systems tracts. Upper Miocene inner-shelf and marginal marine systems tracts and more abundant incised valleys dominate the thinner proximal third-order sequences.

This genetic framework has a major influence on hydrocarbon distribution. Although a strong structural-trapping component is present in the fields, more than 90% of cumulative production originates where fourth-order systems tracts stack to form third-order lowstand systems tracts in all 10 third-order sequences. The development of a high-frequency sequence framework for the prolific Miocene succession and the discovery that hydrocarbons are pooled within the Miocene third-order lowstand systems tracts yield a focused model for the development of abundant undiscovered Miocene reserves in the mature northern Gulf of Mexico shelf province.

AUTHORS

TUCKER F. HENTZ ~ *Bureau of Economic Geology, John A. and Katherine G. Jackson School of Geosciences, University of Texas at Austin, Box X, University Station, Austin, Texas, 78713; tucker.hentz@beg.utexas.edu*

Tucker F. Hentz is a research associate at the Bureau of Economic Geology, University of Texas at Austin, which he joined in 1982. He graduated cum laude with a B.A. degree in geology from Franklin & Marshall College in 1977 and received his M.S. degree in geology from the University of Kansas in 1982. His research interests include the regional sequence stratigraphy of gas-bearing successions in the Anadarko basin, Rio Grande embayment, and Gulf Coast basin.

HONGLIU ZENG ~ *Bureau of Economic Geology, John A. and Katherine G. Jackson School of Geosciences, University of Texas at Austin, Box X, University Station, Austin, Texas, 78713*

Hongliu Zeng has been a research scientist at the Bureau of Economic Geology, University of Texas at Austin, since 1997. His research interests include seismic sedimentology, seismic stratigraphy, and special seismic processing, applied to petroleum prospecting. He earned his B.S. (1982) and M.S. (1985) degrees in geology from the Petroleum University of China and his Ph.D. (1994) in geophysics from the University of Texas at Austin.

ACKNOWLEDGEMENTS

We acknowledge the significant research contributions to this study made by our colleagues, namely, Lesli J. Wood, L. Frank Brown Jr., Michael V. DeAngelo, Adrian C. Badescu, Cem O. Kiliç, and Claudia Rassi. John T. Ames and Jana S. Robinson prepared the figures under the direction of Joel L. Lardon. Susann V. Doenges copyedited the text prior to the submission of the revised draft. Peer reviews by William E. Galloway, James P. Rogers, and Peter K. Webb are greatly appreciated and have improved the manuscript.

This article was prepared with the support of the U.S. Department of Energy (DOE) under Cooperative Agreement No. DE-FC26-98FT40136, with Gary P. Sames as the project

manager. However, any opinions, findings, conclusions, or recommendations expressed herein are those of the authors and do not necessarily reflect the views of the DOE. As an industry partner, Chevron-Texaco contributed the well-log, production, and 3-D seismic data. Landmark Graphics Corporation provided software for display of well-log correlations and interpretation of seismic data via the Landmark University Grant Program. The Owen-Coates Fund of the Geology Foundation, University of Texas at Austin, provided partial support of publication costs. This article was published with the permission of the director of Bureau of Economic Geology, John A. and Katherine G. Jackson School of Geosciences, University of Texas at Austin.

INTRODUCTION

Siliciclastic Miocene strata are currently the most productive of all chronostratigraphic units in the northern Gulf of Mexico's outer continental shelf, accounting for 40% of all hydrocarbons produced and 40% of all remaining proved reserves. Most of these Miocene resources (99% of cumulative production, 61% of remaining proved reserves) are restricted to the present continental shelf (Crawford et al., 2000), where the majority of active fields are considered mature. These statistics indicate that significant potential exists for interfield and intrafield development in the shelf area (<650 ft [198 m] water depth). Moreover, deep Miocene strata (>15,000 ft [4572 m] subsea) below established reservoirs in the shelf area hold promise for additional resources. Only 5% of all wells drilled on the Gulf of Mexico shelf have penetrated strata below 15,000 ft (4572 m), in which there is an estimated 10.5 tcf [297 billion m³] of deep-gas recoverable resources (Minerals Management Service, 2001).

With more than one-third of proven recoverable natural-gas resources of the Gulf of Mexico remaining to be produced from Miocene shelf-bound fields and the potential for new gas resources from the deep Miocene, a need exists for a detailed stratal framework to guide future exploration and production efforts on the modern Gulf of Mexico shelf. Toward this end, we focus on the low- and high-frequency (reservoir-scale) sequence stratigraphy of most of the Miocene series (upper lower Miocene to Pliocene) in the mature Starfak field (designated Vermilion Block 50 field by the Minerals Management Service), nearby Tiger Shoal field, and the surrounding 352-mi² (911 km²) area of 3-D seismic coverage (Figure 1). The approximately 10,000-ft (~3048-m)-thick study interval comprises siliciclastic marine and continental strata that contain more than 60 distinct sandstone-body reservoirs distributed throughout the section. Although abundant well-log and seismic data that image the Miocene succession have been used for decades in the search for hydrocarbons in the Gulf of Mexico, we have not encountered any published examinations of the high-frequency sequence stratigraphy of the series (either local or regional) in offshore Louisiana. Establishment of such a framework based on both detailed well-log and advanced seismic visualization should be a primary focus to effectively develop remaining resources in the mature shelf areas of the Gulf of Mexico.

The objectives of this article are to (1) document the low- (third-order) and high-frequency (fourth-order) sequence-stratigraphic framework of the Miocene succession within the study area, providing a basis for the framework's extrapolation into the extensive Miocene play fairways surrounding the study area (Hunt and Burgess, 1995; Seni et al., 1997) and into strata having potentially deep (lower Miocene) production and (2) address the regional sequence-stratigraphic context of resource distribution within the Miocene succession in the field areas. The ultimate intent is to provide explorationists with additional tools and insight to help develop the

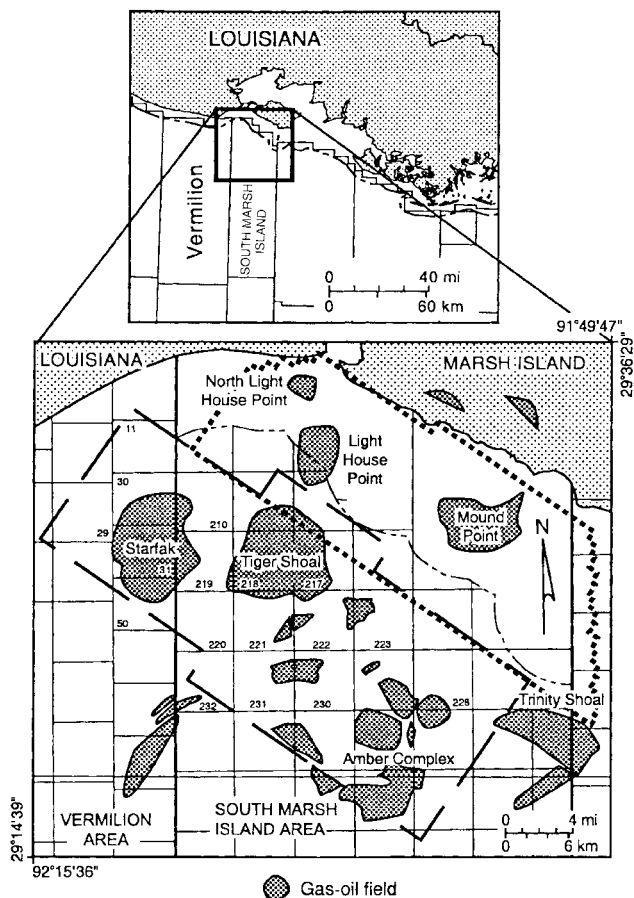


Figure 1. Map of study area within Vermilion and South Marsh Island areas, offshore south-central Louisiana, showing areas of well-log coverage (Starfak and Tiger Shoal fields) and outlines (dashed lines) of two 3-D seismic surveys used in the study.

voluminous untapped Miocene resources of the mature Gulf of Mexico shelf.

Database

All data from Starfak and Tiger Shoal fields were provided by Texaco Exploration and Production (New Orleans office). Data pertinent to this article consist of wireline logs for all 156 wells in the two fields, each well's complete production and engineering history, biostratigraphic reports for 15 wells within both fields, and a 3-D seismic survey (acquired in 1994 and 1995) covering 352 mi² (912 km²). Starfak and Tiger Shoal fields lie in the northwest half of the seismic survey (Figure 1). Although McBride et al. (1988) indicated the existence of three whole cores from Starfak field, we have not been able to locate them for first-hand description. However, depositional, petrographic, and paleontologic aspects of one of these cores from the deep (14,780–14,862 ft [4505–4530 m]) *Robulus* L

zone is described in an internal Texaco report. Moreover, Hart et al. (1989) described the same core and another slightly shallower one taken from the same well (Texaco No. 6, Vermilion Block 31).

Most maps and cross sections that we present illustrate sequences and systems tracts in Starfak field, which was discovered almost two decades after Tiger Shoal field and is thus represented by higher quality well logs having more log curves, notably the gamma-ray log. Moreover, the Starfak sections are cut by markedly fewer faults with smaller apparent offsets. However, differences in data quality are minor and did not adversely impact interpretations.

PREVIOUS WORK

Since the early 1980s, stratigraphic analysis of the Miocene series of the northern Gulf of Mexico has focused on the regional-scale depositional history (e.g., Winker, 1982; Galloway et al., 1986; Morton et al., 1988), genetic stratigraphy of low-frequency cycles (Galloway, 1989; Galloway et al., 2000), and definition of primarily low-order sequences based on basin-wide correlation of biozones (Styzen, 1996; Lawless et al., 1997; Fillon and Lawless, 1999, 2000). Play atlases of the northern Gulf of Mexico (Bebout et al., 1992; Seni et al., 1997) classify Miocene reservoir-bearing strata within broad groupings based on chronozone and depositional style. In all these approaches, however, details of the genetic stratal architecture, systems tracts, and the pattern of hydrocarbon distribution within this framework were beyond their scope. These topics will be addressed here.

Published studies of Starfak and Tiger Shoal fields do not exist, and there is a paucity of detailed lithostratigraphic, sequence-stratigraphic, and structural data for the Miocene series near the study area. Van Wagoner et al. (1990) presented a regional cross section of middle Miocene fourth-order sequences of onshore south-central Louisiana. However, the authors cited no published study for this work to enable access to primary data. Using seismic data, Wagner et al. (1994) examined the lower Miocene sequence stratigraphy of the nearshore West Cameron and East Cameron areas in the Federal Outer Continental Shelf approximately 25 mi (~40 km) west of Starfak field. Wells in Starfak and Tiger Shoal fields do not penetrate the part of the lower Miocene examined by these authors; however, we do have seismic coverage of the lower Miocene in our study area, and their conclusions were useful in our

deep seismic interpretation. Luo (2000), who studied the same 3-D seismic data set in her thesis work, provided insight into the regional history of growth-fault development. Paleontologic studies of foraminiferal abundances (Rosen and Hill, 1990), general calcareous nannofossil diversity (Jiang and Watkins, 1992; Jiang, 1993), and basin-scale faunal zones (Lawless et al., 1997) of the northern Gulf of Mexico provided critical constraints on absolute ages of the Miocene succession in Starfak and Tiger Shoal fields.

STRUCTURAL CONTEXT

The study area (Figure 1) is located in the Oligocene–Miocene Detachment Province of the northern Gulf Coast continental margin (Diegel et al., 1995). This region is generally characterized by large-displacement, dominantly down-to-the-basin, listric growth faults that sole on a regional detachment zone above the Oligocene section. Regional deformation either is a product of salt mobilization from the level of the autochthonous Jurassic Louann Salt, or it is a result of detachment and growth-fault development along a salt weld that formerly contained a thick, allochthonous salt body (Diegel et al., 1995; Luo, 2000). A characteristic feature of this province is the great thickness of deltaic and other on-shelf sediments above the detachment zone, typically exceeding 3 mi (5 km). This remarkable succession of thick Miocene on-shelf, shelf-edge, and slope siliciclastics accumulated during a period of generally high sedimentation rates. These sediments were generated by rejuvenation of continental highlands, particularly the southern Appalachians during the middle to late Miocene (Boettcher and Milliken, 1994; Galloway et al., 2000) and help make this region one of the world's great high-quality petroleum reservoir provinces. Starfak and Tiger Shoal fields lie within the heart of this region.

Geologic conditions in the greater two-field study area are structurally simple compared to those of the complex, diapirically deformed strata that occur to the south. The two fields are associated with several sub-regional first-order normal growth faults and associated second-order ancillary faults, the latter of which cause additional structural partitioning within the fields (Figure 2). First-order growth faults are characterized by large apparent offsets (>500 ft [152 m]), and they extend from near the sea floor to below the maximum depth of our seismic coverage (4.4 s, ~18,000 ft [~5486 m]), probably soling out in the lowermost

Miocene. Second-order faults occur with both growth and nongrowth geometries and in typically much shorter segments with less apparent offset. However, the magnitude of fault disruption is minor in the areas of well control, our 3-D seismic database is excellent, and well-log quality is good, all allowing optimal analysis of high- and low-order sequence cyclicity in this area of the northern Gulf of Mexico.

RESERVOIR FRAMEWORK

Starfak and Tiger Shoal fields produce hydrocarbons from sandstones throughout most of the Miocene Series (upper lower through upper Miocene), which in the study area forms a dominantly regressive succession as much as approximately 10,000 ft (~3048 m) thick (Figure 3). The study area lies within part of the ancestral Mississippi River depocenter (McGookey, 1975), most recently designated the Central Mississippi sediment-dispersal axis by Galloway et al. (2000). This upward-shallowing trend of depositional facies is widely present in the Miocene-shelf interval of the offshore northern Gulf of Mexico (Seni et al., 1997).

Although surfaces on or within many of the Texaco-designated reservoir sandstones typically coincide with key sequence-stratigraphic boundaries, vertical reservoir boundaries are nongenetic. In accordance with Texaco's established nomenclature, these sandstone-body reservoirs are designated (in descending order) A through Z sands (some are variously subdivided using alphanumeric designations, such as T-1 sand and M-1 [lower] sand), 12000 A sand, 12000 B sand, and the *Robulus* L-1 through *Robulus* L-8 sands (Figure 3). Reservoir sandstones range in depth from approximately 6200 to 16,200 ft (~1890 to 4938 m) in Starfak field and from approximately 6000 to 15,400 ft (1829 to 4694 m) in Tiger Shoal field. The two fields are currently operated by Chevron-Texaco. Tiger Shoal has produced gas and oil from 103 wells and was discovered in 1958, whereas Starfak field, discovered in 1975, comprises 53 wells, mostly gas producers. Sixty-two gas and oil reservoirs lie within Starfak and Tiger Shoal fields: 15 in Starfak and 47 in Tiger Shoal.

SEQUENCE-STRATIGRAPHIC FRAMEWORK

The sequence-stratigraphic interpretation techniques used in this study are discussed in Van Wagoner et al. (1990) and Mitchum et al. (1993). This approach en-

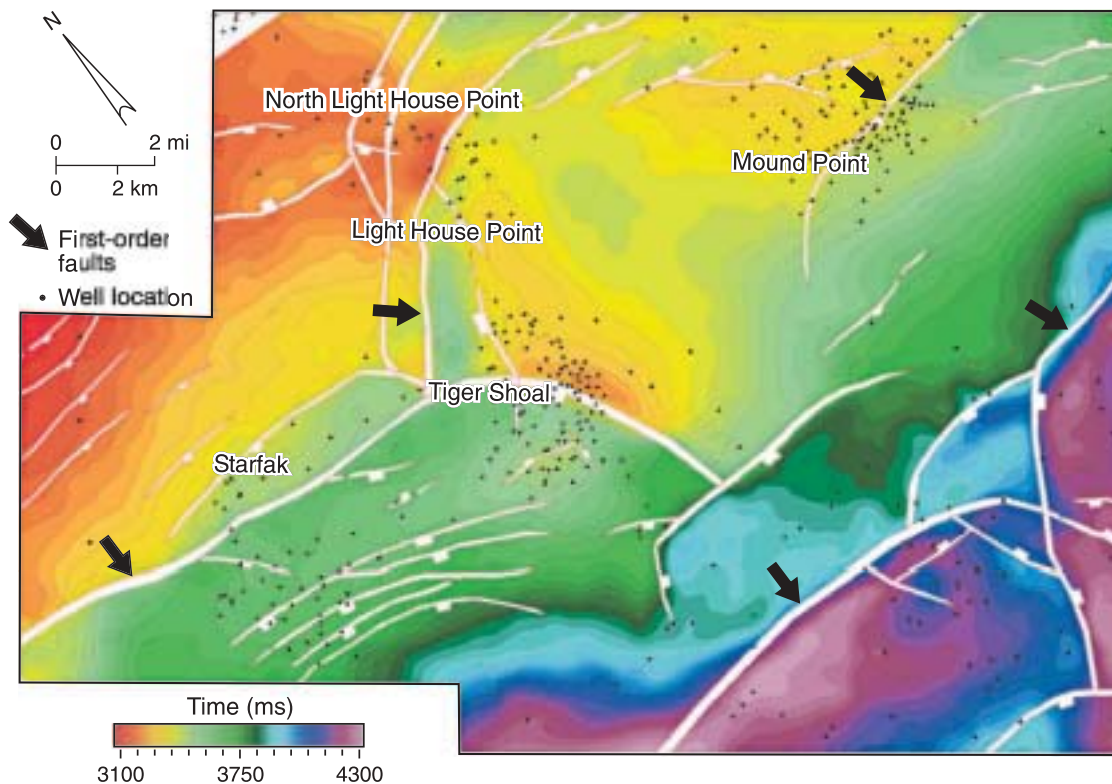


Figure 2. Time-structure map of an upper lower Miocene fourth-order maximum flooding surface (MFS) from the study interval. Structure is dominated by first-order growth faults (>500 ft [152 m] of apparent offset) and smaller second-order ancillary faults. Contour interval is 25 ms. Area coincides with that of the seismic surveys shown in Figure 1.

abled construction of a genetic context for all phases of our study of the Miocene succession (Hentz et al., 2000, 2001, 2002; Zeng et al., 2000, 2001a, b, c; Badescu and Zeng, 2001; DeAngelo and Wood, 2001; Rassi and Hentz, 2001; Zeng, 2001; Dutton and Hentz, 2002; Rassi, 2002; Zeng and Wood, 2002). Moreover, it establishes the groundwork for investigations of reservoir-specific attributes and the identification of previously undetected hydrocarbon resources within the two-field area, this study's 3-D seismic volume, and adjacent on-shelf areas.

Biostratigraphy

Faunal data from unpublished Texaco paleontologic reports from 15 wells in both fields indicate that the approximately 10,000-ft (~3048-m) section from the oldest reservoir (*Robulus* L-8 sand) at the base of the study interval to the Pliocene/Miocene boundary just above the uppermost reservoir (A sand) represents approximately 11.2 m.y. of deposition. The study interval ranges in age from latest early Miocene (late Burdigalian, ~17.3 Ma) to the end of the Miocene (early

Messinian, ~6.1 Ma). We employ the Miocene stage boundaries used by Texaco: the extinction horizons of *Robulus* L (top of lower Miocene), *Cibicides carstensi* (top of middle Miocene), and *Robulus* E (top of upper Miocene) (R. G. Lytton III, 2001, personal communication). Fourteen regional Gulf of Mexico foraminiferal biozones (Picou et al., 1999) occur within the study interval, ranging from the *Cibicides* 38 and *Robulus* L zones (~16.5 Ma) to the *Robulus* E zone (~6.1 Ma) at the top of the Miocene series. However, lower Miocene strata in deep wells in nearby North Light House Point and Mound Point fields (Figure 1) record the regional *Operculinoides* zone (extinction horizon of *Robulus* 54-B), the next oldest regional Gulf of Mexico biozone (at ~18.0 Ma), occurring at approximately 600–700 ft (~183–213 m) below the base of the deepest well-log section in the two study fields. Ages of regional biozones in our study were initially derived from Lawless et al. (1997), who used the time-scale of Berggren et al. (1985); we converted these ages to the revised chronology of Berggren et al. (1995).

In most instances, the top of each regional biozone is chronostratigraphically well constrained in Starfak

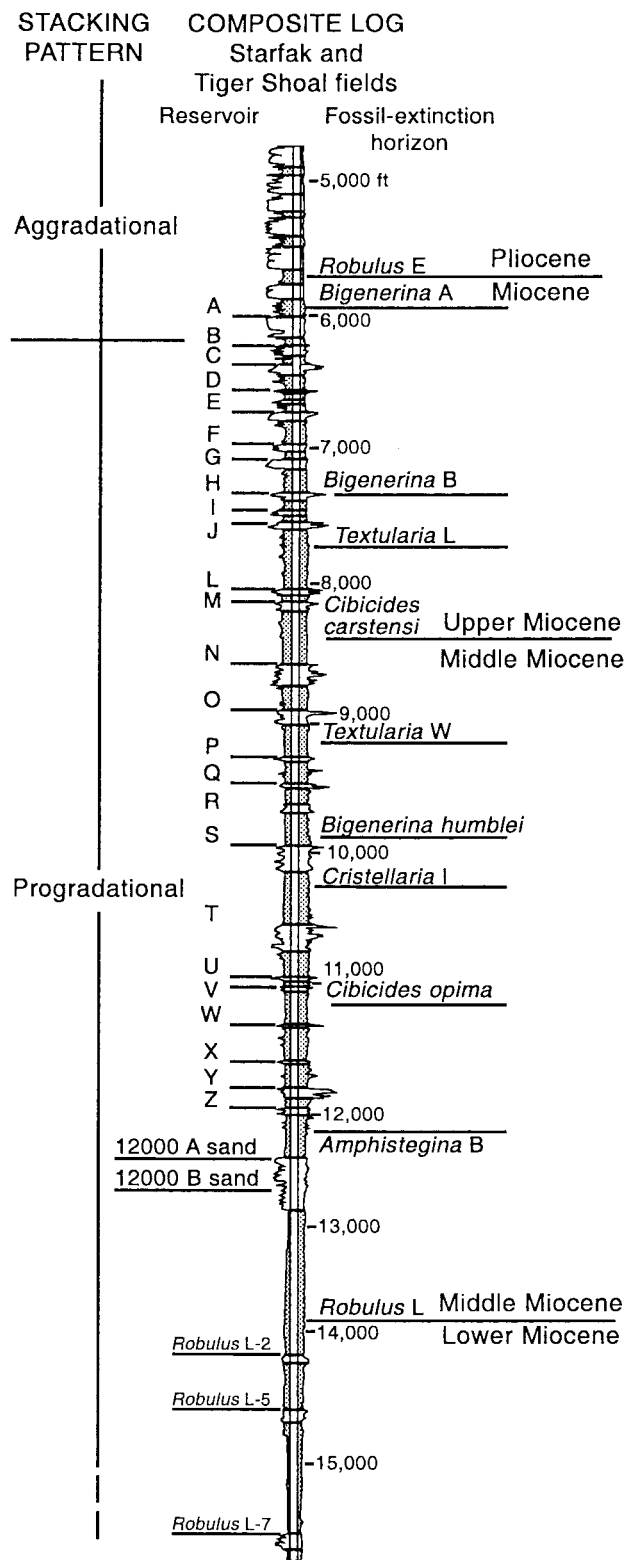


Figure 3. Composite representative log of Starfak and Tiger Shoal fields displaying gross stacking patterns, reservoir nomenclature, extinction horizons of major Gulf of Mexico biomarkers, and stage boundaries.

and Tiger Shoal fields, with approximately 40–100 ft (~12–30 m) of vertical variance for the top of each zone among the 15 wells having fossil data. These zones consistently extend across the same flooding shales in the 15 wells. However, the variation in the highest occurrences of *Cibicides opima* and *Bigenerina B* (within shales and overlying sandstones) is not as well constrained, most likely because of changing environmental conditions causing pronounced changes in depositional facies. Highest occurrences of both taxa within sandstones may also be a result of redeposition of fossils above unconformities. Owing to this uncertainty in the positions of extinction horizons, these biozones are depicted within chronostratigraphic ranges.

Paleobathymetric indicator fauna, benthic organisms that lived within certain ranges of water depth (Picou et al., 1999), enabled reconstruction of water depths during deposition of reservoir-scale (fourth-order) systems tracts (Table 1). Several of the Texaco paleontologic reports include complete faunal-count lists recorded by the well-site paleontologists. In most wells, samples were recorded every 30 ft (9 m) from immediately above the study interval to total depth. These lists provide an accounting of fossil assemblages, abundances of individual species, and stratigraphic positions of major faunal “floods.” Indicator fossils within faunal floods, which typically coincide with our marine condensed sections, can be used to estimate the paleobathymetric conditions under which the sediments containing the fossils were deposited. The indicator fossils record an overall upward-shallowing trend within the entire study interval (Figure 4), coinciding with the overall regressive stratal-stacking pattern. Information provided by the indicator fossils also offers corroborative evidence for our interpretations of systems tracts, which are discussed in following sections.

Sequence Interpretation

The approximately 10,000-ft (~3048-m) Miocene succession in Starfak and Tiger Shoal fields comprises 10 third-order sequences and no fewer than 58 fourth-order sequences, which average approximately 1.1 and 0.19 m.y. in duration, respectively. The average duration of our third-order sequences, composed of fourth-order sequence sets (Mitchum and Van Wagoner, 1990), is comparable to that of the Miocene Series measured in basins worldwide (Haq et al., 1988; Hardenbol et al., 1998). The average duration of our fourth-order sequences is also comparable to that of other Miocene fourth-order sequences of the Gulf

Table 1. Characteristic Paleobathymetric Indicator Fossils (Foraminifera) in the Miocene Section of Starfak and Tiger Shoal Fields (modified from Picou et al., 1999).

Marginal marine
<i>Ammonia beccarii</i>
<i>Elphidium</i> spp.
Inner neritic (0–60 ft [0–18 m])
<i>Bifarina vicksburgensis</i>
<i>Buccella hannai</i>
<i>Buccella mansfieldi</i>
<i>Cibicides concentricus</i>
<i>Eponides</i> spp.
<i>Nonionella</i> spp.
<i>Reusella</i> spp.
Middle neritic (60–300 ft [18–91 m])
<i>Bolivina floridana</i> (uncommon)
<i>Cancris sagra</i>
<i>Cibicides carstensi</i>
<i>Cibicides floridanus</i>
<i>Gyroidina hannai</i>
<i>Uvigerina peregrina</i> (uncommon)
Outer neritic (300–600 ft [91–183 m])
<i>Ammobaculites nummus</i>
<i>Bolivina floridana</i> (common to abundant)
<i>Chilostomella</i> spp.
<i>Cibicides opima</i>
<i>Gaudryina atlantica</i>
<i>Gyroidina scalata</i>
<i>Liebusella</i> spp.
<i>Pullenia salisburyi</i>
<i>Textularia barretti</i>
<i>Uvigerina altacostata</i> (uncommon)
<i>Uvigerina carapitana</i>
<i>Uvigerina howei</i>
<i>Uvigerina lirettensis</i>
<i>Uvigerina peregrina</i> (common to abundant)
<i>Valvulinaria</i> spp.
Upper bathyal (600–1500 ft [183–457 m])
<i>Anomalina alazanensis</i>
<i>Cibicides matanzanensis</i>
<i>Cyclammina cancellata</i>
<i>Liebusella pozonensis</i>
<i>Planulina harangensis</i>
<i>Uvigerina altacostata</i> (common to abundant)

Coast Basin (Van Wagoner et al., 1990). Because our data set does not allow observation of the full shelf-to-basin profile of the Miocene sequences, relative positions of coastal onlap can only be inferred. How-

ever, the third-order sequences exhibit an upward-thinning trend (Figure 5), the upsection occurrence of progressively shallower water benthic-fossil assemblages (Figure 4), decreasing fossil abundance and diversity (Figure 5), and a generally upward thinning of lowstand systems tracts, collectively indicating the progressive upsection coastal offlap of the Miocene succession.

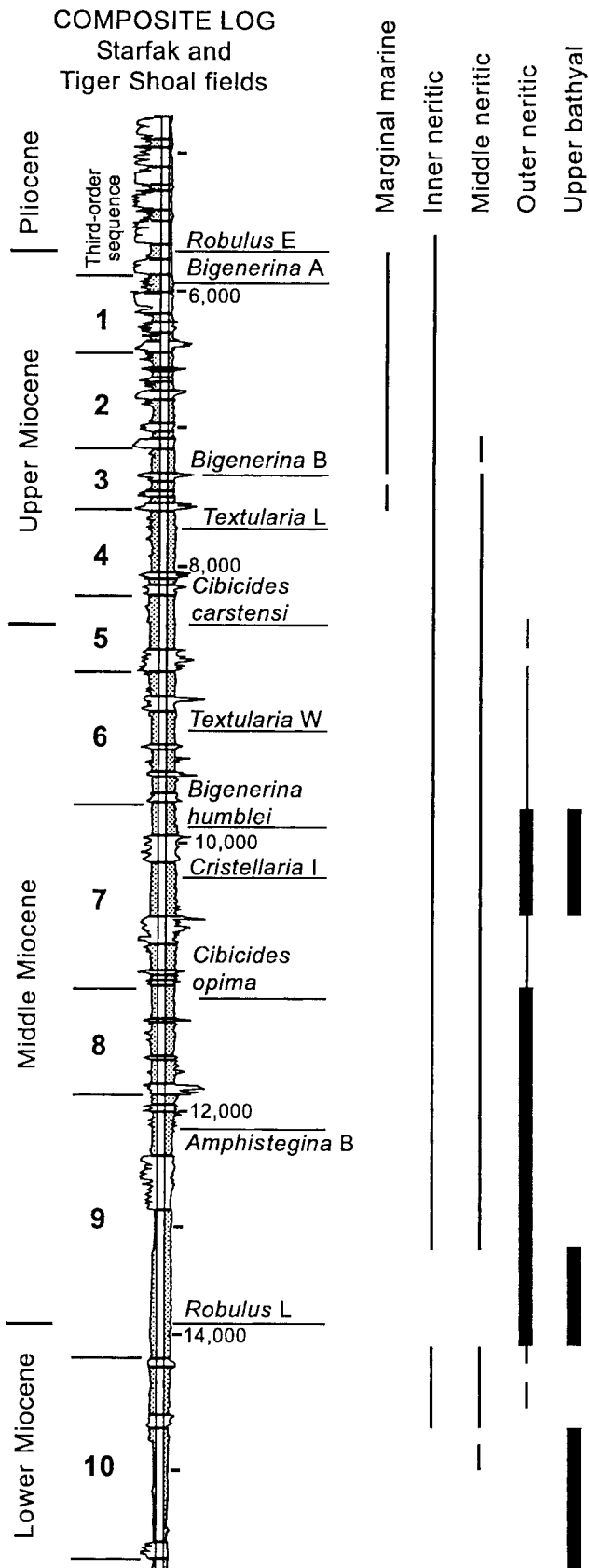
Conceptually, stratal stacking patterns within third-order systems tracts vary relative to their position in the shelf-to-basin depositional profile (Mitchum and Van Wagoner, 1990; Mitchum et al., 1993). Furthermore, these variations coincide with changes in stratal attributes of the component fourth-order systems tracts. Therefore, we subdivided the study interval into distal, medial, and proximal third-order sequences, based on their relative positions in a generalized Miocene shelf-to-basin depositional profile (Figure 6), to systematically document larger scale stratal and depositional trends within the approximately 10,000-ft (~3048-m) study interval.

Distal Sequences (SB 10 to SB 8)

Stratal Characteristics

Third-order sequences 10 and 9 (lower and middle Miocene) extend from sequence boundary (SB) 10 near the base of the study interval to SB 8, just above the regional *Amphistegina* B biozone (Figures 7, 8). The sequences are comparable in thickness, ranging between approximately 1600 and 1800 ft (~488 and 548 m) respectively. Both sequences are characterized by thick (as much as ~1100 ft [~335 m]) shale-dominated sections in their lower parts. These thick basal shales contain periodic, interbedded shaly sandstones within thin zones of several tens of feet that exhibit both upward-fining and upward coarsening trends. The basal contact of sequence 10 differs from that of sequence 9 by exhibiting thick (each as much as ~250 ft [~76.2 m]) single or multiple, blocky-serrate, aggradational sandstone units that record little or no incision (Figure 7, ~15,700–15,900 ft [~4785–4846 m] in Texaco No. 3).

In both sequences, the thick basal shale interval is overlain by a series of interstratified upward coarsening, progradational shale-and-sandstone units, totaling approximately 580–770 ft (~152–235 m), with each unit as much as approximately 200 ft (~61 m) thick. Thin (as much as ~40 ft [~12 m]), typically weakly developed retrogradational shale sections overlie the progradational units. These progradational-



retrogradational pairs stack to form a progradational set characterized by a general upsection trend of coarsening sandstones (the *Robulus L* sands of Texaco) within the pairs (Figure 7, ~14,200–14,930 ft [~4328–4551 m] in Texaco No. 3; Figure 8, ~12,780–13,500 ft [~3895–4115 m] in Texaco No. 4). In their study of whole core from the equivalent interval in another Starfak well, Hart et al. (1989) also recognized this overall regressive trend from paleoecologic data. The upper progradational units of both progradational sets within the two sequences either are capped by thin (as much as ~25 ft [~8 m]), but locally well-developed, sandstones above dominant shale (Figure 7, particularly at ~14,300–14,440 ft [~4359–4401 m] in Texaco No. 3) or occur as gradually upward coarsening, sandstone-dominated units (Figure 8, at ~12,780–12,920 ft [~3895–3938 m] in Texaco No. 9). Unlike sequence 10, sequence 9 contains blocky, blocky-serrate, and more uncommonly, upward-fining aggradational sandstone units as thick as 120 ft (37 m) (Figure 8, ~13,000 ft [~3962 m]) within this progradational set. These units have sharp erosional bases that incise correlated shale marker beds.

Also in marked contrast to sequence 10, the upper part of sequence 9 comprises a second progradational set of stacked upward coarsening units (Figure 8, ~12,330–12,820 ft [~3758–3907 m] in Texaco No. 17). A thin (~10–50 ft [3–15 m]) retrogradational interval overlies each upward coarsening unit. The set ranges from approximately 400 to 500 ft (~122 to 152 m) in thickness, with each unit ranging from approximately 60 to 160 ft (~18 to 49 m) in thickness.

Systems Tracts

All of third-order distal sequence 10 and the lower two-thirds of sequence 9 represent third-order low-stand slope-fan and prograding complexes (Figure 6).

Figure 4. Ranges of paleobathymetric zones recorded within the study interval. The widest parts of zone bars represent stratigraphic intervals of particularly abundant indicator fauna. Many sandstones and immediately subjacent shaly strata in the lower two-thirds of the study interval were deposited under marginal marine conditions; however, indicator fossils of this environment are sparsely preserved. Marginal marine = shallow, brackish conditions; inner neritic = approximately 0–60 ft (~0–18 m); middle neritic = approximately 60–300 ft (~18–91 m); outer neritic = approximately 300–600 ft (~91–183 m); and upper bathyal = approximately 600–1500 ft (~183–457 m). Lists of indicator fossils used in this study are from Picou et al. (1999).

Basin-floor-fan sandstones also occur at the base of sequence 10. Well-log expressions of these lowstand divisions conform to those described in Mitchum et al. (1990, 1993). Benthic paleofauna indicate that the third-order lowstand systems tracts in the two sequences represent overall upward-shallowing successions that

range from basin-floor and lower and upper slope (upper bathyal) deposits at the base to inner-shelf (marginal marine to middle-neritic) facies at the top (Figures 4, 7, 8). The third-order SB of sequence 10 (Figure 7, at ~15,760 ft [~4785 m] in Texaco No. 4 and ~15,890 ft [~4843 m] in Texaco No. 3) coincides with the base of a thick blocky-serrate basin-floor-fan sandstone deposited in an upper bathyal environment. The base of another well-developed basin-floor-fan sandstone approximately 150–200 ft (~46–61 m) below SB 10 (Figure 7, at ~16,150 ft [~4922 m] in Texaco No. 3) in a few deep wells may represent another third-order SB near the distal margin of an older fan deposit.

The thick shale intervals in the lower parts of sequences 10 and 9 represent outer-neritic to upper bathyal (Figure 4) slope-fan deposits. Sandy zones within them probably record mid-slope turbidites and shingled turbidite channel/levee deposits that mark fourth-order clinoform toes (Erskine and Vail, 1988) or fourth-order basin-floor fans (Mitchum et al., 1993). We could not systematically correlate possible fourth-order sequence boundaries through the slope-fan deposits where progradational intervals are not consistently well defined. Mitchum and Van Wagoner (1990) proposed that sequence boundaries are not easily recognized in third-order slope fans because they have no shallow-marine equivalents.

Fourth-order sequence boundaries of the sequence 10 prograding complex coincide with the bases of upward coarsening, prograding-wedge sandstone/shale units (top of sequence) deposited in marginal marine to middle/outer-neritic environments. Hart et al. (1989) noted a mix of terrestrial, estuarine, and marine paly-nomorphs in whole cores from two of the fourth-order prograding wedges in sequence 10 (second and fifth wedges from the base in Figure 7). They interpreted the depositional setting of the sandstones as outer-neritic shelf, possibly storm or deltaic deposits,

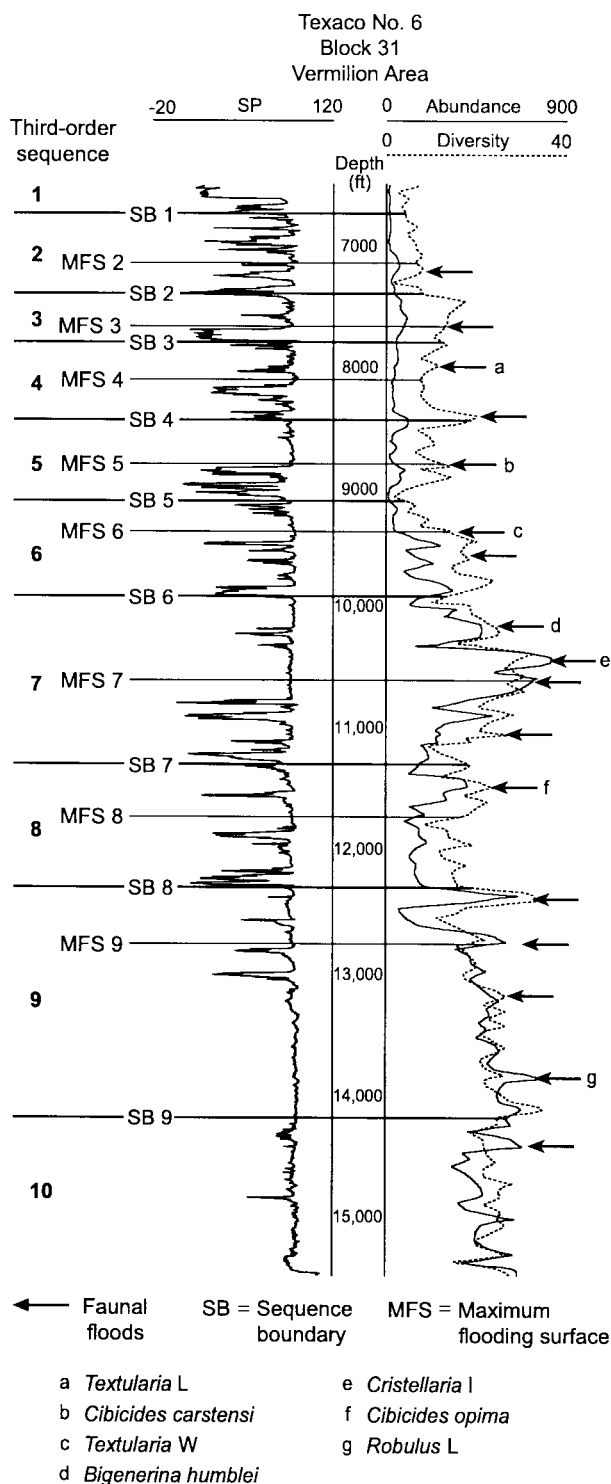


Figure 5. Third-order sequence boundaries and MFSs and representative curves of total foraminiferal abundance and diversity within the study interval. The chronostratigraphic positions of depicted major and minor faunal “floods,” derived from fossil summaries of paleontologic reports from 15 wells from Starfak and Tiger Shoal fields, are very consistent among wells. Regional Gulf of Mexico biozones that coincide with floods are also depicted. Note that most third-order MFSs coincide with faunal floods; other floods mark prominent fourth-order MFSs. MFS 1 (not shown) coincides with the *Bigenerina A* extinction horizon (Figure 22).

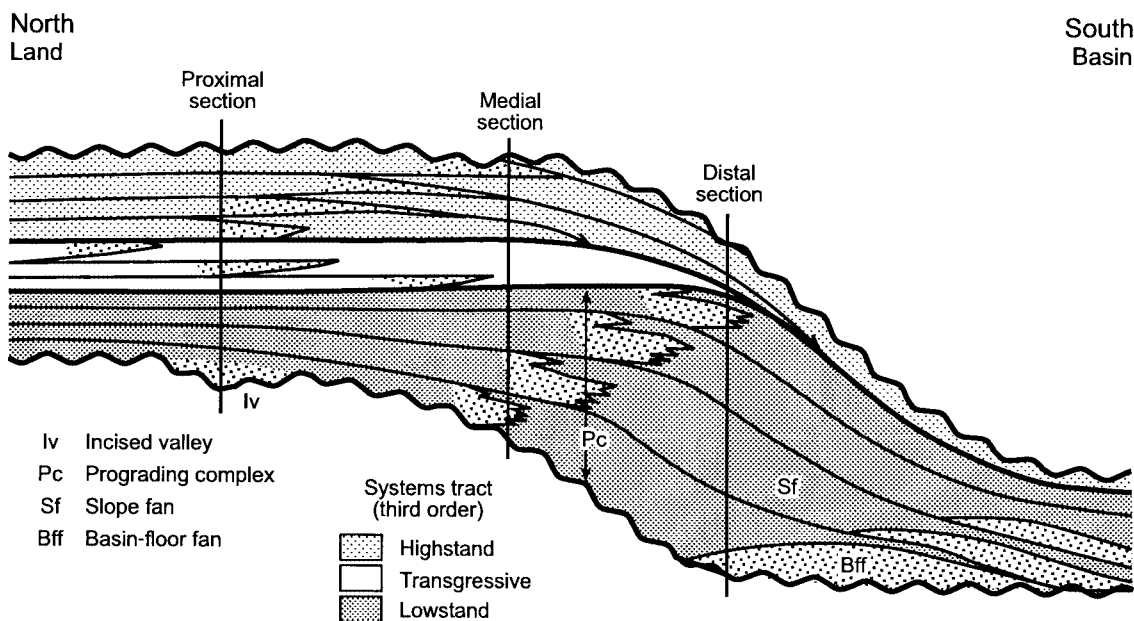


Figure 6. Relative positions of distal, medial, and proximal third-order sequences and systems tracts in a schematic Miocene shelf-to-basin depositional profile. The Miocene study interval comprises two distal, four medial, and four proximal third-order sequences.

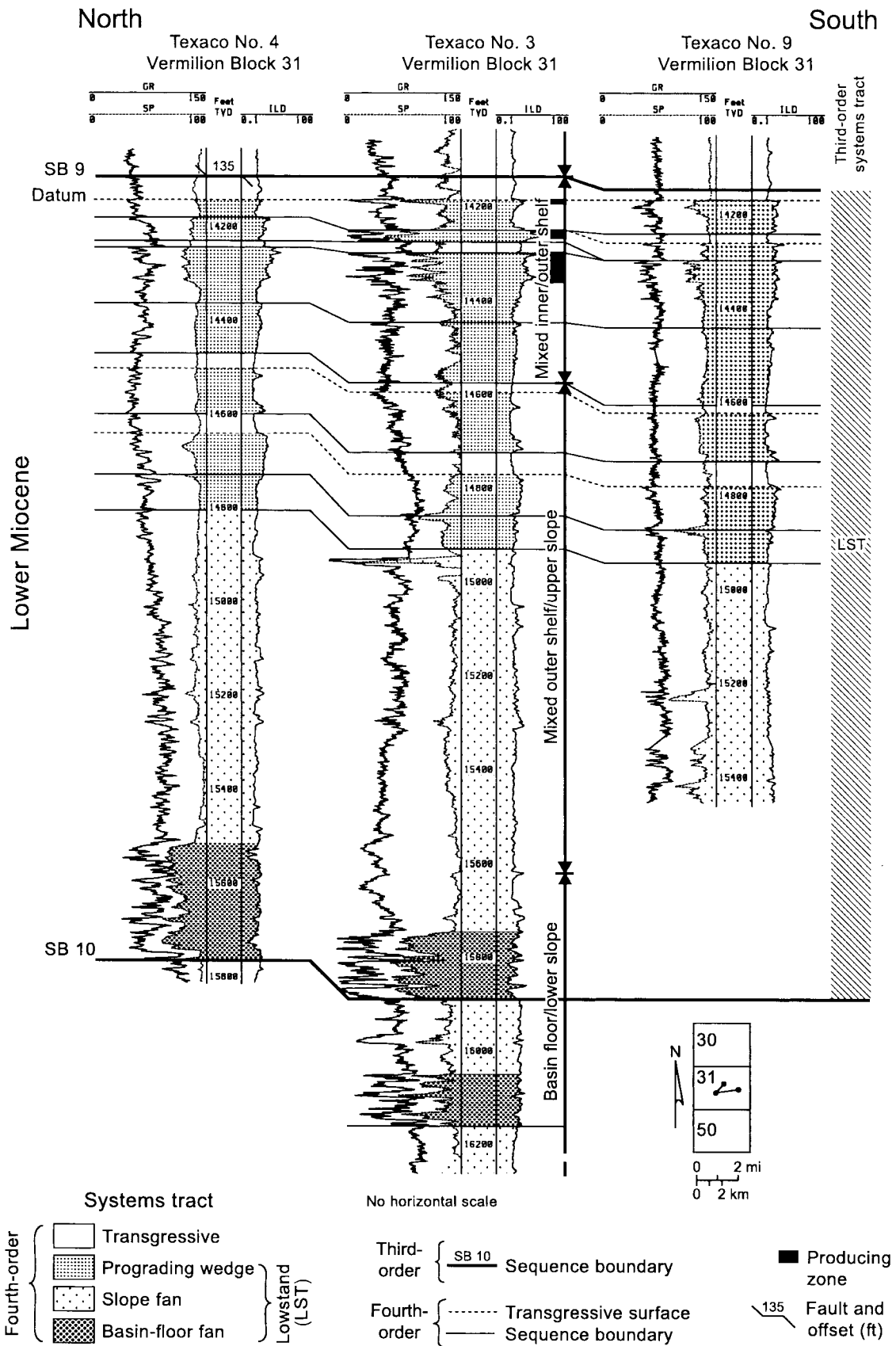
but inferred no sequence-stratigraphic context. An internal Texaco report of the lower core from the same well (interpreted in Dutton and Hentz, 2002) ascribed a similar depositional/paleobathymetric setting. We concur with a deltaic setting but conclude that the progradational units represent a range of marginal marine (sandy top) to possible middle-neritic (shaly base) water depths. Seismic imaging of the sandier upper parts of the prograding complexes in distal and medial sequences by amplitude stratal slicing (Zeng et al., 2001a) shows that fourth-order wedges are as much as 10 mi (16 km) in strike width and more than 3 mi (5 km) in the dip dimension (Figure 9). Third-order prograding complexes (sequence sets) are only marginally wider along depositional strike (as much as approximately 12 mi [~19 km]), indicating focused lowstand deltaic deposition within the third-order (1.1 m.y.) time frame. These dimensions contrast markedly with the much greater

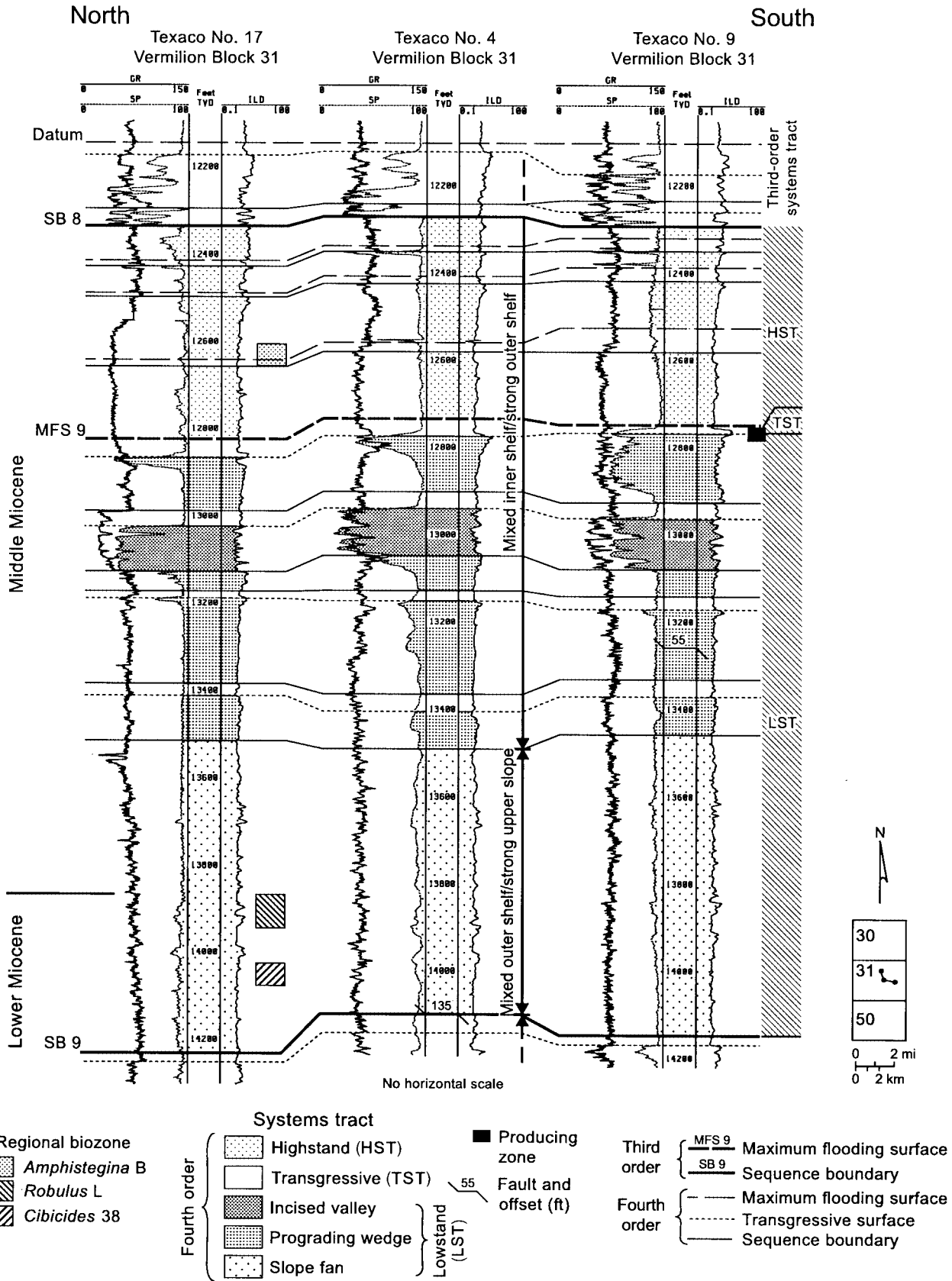
areal dimensions of the highstand deltas (discussed in “Medial Sequences”).

The sequence 9 third-order prograding complex contains inferred incised-valley fills (blocky sandstones) and generally better developed fourth-order prograding-wedge sandstones (than those in sequence 10) in the upper part (Figures 8, 9). No basin-floor-fan sandstones occur at the base of sequence 9. Moreover, unlike sequence 10, the upper third of sequence 9 comprises a well-developed sequence set of fourth-order highstand and transgressive systems tracts that represents the third-order highstand systems tract, which was deposited in marginal marine to outer-neritic water depths. These features all indicate a more proximal position for sequence 9 relative to that of sequence 10.

The inferred third-order transgressive systems tract and the MFS of sequence 9 that coincides with a major faunal flood (Figure 5) immediately overlie the third-order lowstand systems tract (Figure 8). Relative to the

Figure 7. Dip cross section of distal third-order sequence 10 (lower Miocene), Starfak field, representing the most distal of third-order systems tracts. Third-order transgressive and highstand shales probably exist in uppermost sequence 10; however, consistent well-to-well-log patterns identifying these deposits are not evident. Fourth-order prograding-wedge sandstones compose the hydrocarbon reservoirs. Only three wells penetrate this deep zone in Tiger Shoal field because prospective prograding-wedge sandstones are poorly developed there. In the thick shale intervals, grain-size trends are best recorded by the deep induction log (ILD). Because of casing of shales in the borehole, the gamma-ray log is an unreliable record of lithology and grain-size trends in these deep zones. Paleobathymetric interpretations are based on benthic fossil assemblages: basin and slope = upper bathyal; outer shelf = outer neritic; and inner shelf = middle neritic to marginal marine (Table 1). Log curves shown are gamma ray (GR), spontaneous potential (SP), and deep induction (ILD).





third-order transgressive systems tracts of most overlying, more proximal sequences, this unit is thin (as much as 40 ft [12 m] thick) because of its distal position. Although distal, shaly transgressive and highstand deposits probably overlie the lowstand progradational complex of sequence 10 (near SB 9), we could not clearly identify them from the well-log expression. Transgressive systems tracts are expressed as a retrogradational (upward-fining, upward-thinning) pattern on gamma-ray, spontaneous-potential, and resistivity logs. The top of the retrogradational log pattern commonly coincides with a high-gamma-ray marker, the position of the MFS. In the distal sequences, the transgressive systems tracts are typically thin and shaly and cannot be confidently distinguished from distal highstand deposits. Retrogradational log patterns of transgressive systems tracts are more clearly discernible in the medial and proximal sequences.

Medial Sequences (SB 8 to SB 4)

Stratal Characteristics

Medial third-order sequences 8 through 5 (middle to upper Miocene, SB 8 to SB 4) range from approximately 600 to 1800 ft (~183 to 548 m) in thickness and extend from approximately 300 ft (~91 m) above the regional *Amphistegina* B biozone to approximately 75 ft (~23 m) above the *Cibicides inflata* biozone (Figures 10–13). Each of the medial sequences comprises three distinct stratigraphic divisions: (1) a lower succession of two to five aggradational (~40–250 ft [~12–76 m] thick) or progradational (~50–180 ft [~15–55 m] thick) units; (2) an atypically thick (~70–190 ft [~21–58 m]), upward-fining, retrogradational, shale-dominated section in the middle; and (3) an upper section of typically two to four (50–500 ft [15–152 m] thick) mostly progradational units of thicker shales and sandstones. Progradational and aggradational units in the lower and upper divisions are interstratified with thinner (~15–50 ft [~5–15 m]) shaly retrogradational intervals. Erosionally based blocky, blocky-serrate, and upward-fining sandstone units (~40–250 ft [~12–76 m] thick) are more common in the lower succession, whereas upward coarsening sandstone/shale units dominate the upper division.

Unlike those of the distal successions, the basal third-order sequence boundaries of the medial sequences are locally marked by pronounced erosional contacts overlain by these sharp-based aggradational sandstone units. In other areas, the basal contacts are conformable, correlating from erosional bases of the sandstone units to the tops of upward coarsening progradational units. In the lower two medial sequences, erosional contacts also correlate with conformable to slightly erosional bases of thick (as much as ~250 ft [~76 m]), typically upward coarsening intervals (only shown in Figure 11, e.g., ~11,000–11,850 ft [~3353–3612 m] in Houston Oil & Minerals No. 5). These progradational intervals are restricted to the downdip part of the area of well control, and their occurrence coincides with marked thickening of the third-order sequence. They differ from the progradational units in the updip areas by being thicker and containing a higher percentage of sandstone, typically composing gradually upward coarsening, sandstone-dominated units with no prominent shale base. In marked contrast to the distal sequences, a thick basal upper-bathyal to outer-neritic shale is not present in the medial sequences.

The middle retrogradational unit only uncommonly contains sandstone beds, which primarily occur in wells from the updip (northern) parts of the sequences (Figure 10, unit below MFS 8).

In the upper division, the progradational/retrogradational pairs stack to form a progradational set characterized by a general upsection trend of increasing sandstone grain size, bed thickness, and number of sandstone beds within the pairs.

Systems Tracts

The lower, middle, and upper stratigraphic divisions of the medial sequences represent third-order lowstand, transgressive, and highstand systems tracts, respectively, that accumulated in upper slope/outer shelf to fluvial environments in marine water depths that ranged from upper bathyal to marginal marine, as indicated by fossil data (Figures 4, 10–13). Two to five relatively thin (~75–100 ft [~23–30 m]) closely spaced fourth-order sequences form the lowstand systems tract. The third-order lowstand systems tract is overlain by the third-order transgressive systems tract, an atypically

Figure 8. Dip cross section of distal third-order sequence 9 (lower and middle Miocene), Starfak field. Producing zones occur in fourth-order prograding-wedge and incised-valley-fill sandstones of the third-order lowstand systems tract. Biozone “boxes” record vertical variance for the top of each zone among the wells with fossil data. Paleobathymetric interpretations are based on benthic fossil assemblages: upper slope = upper bathyal; outer shelf = outer neritic; and inner shelf = middle neritic to marginal marine (Table 1).

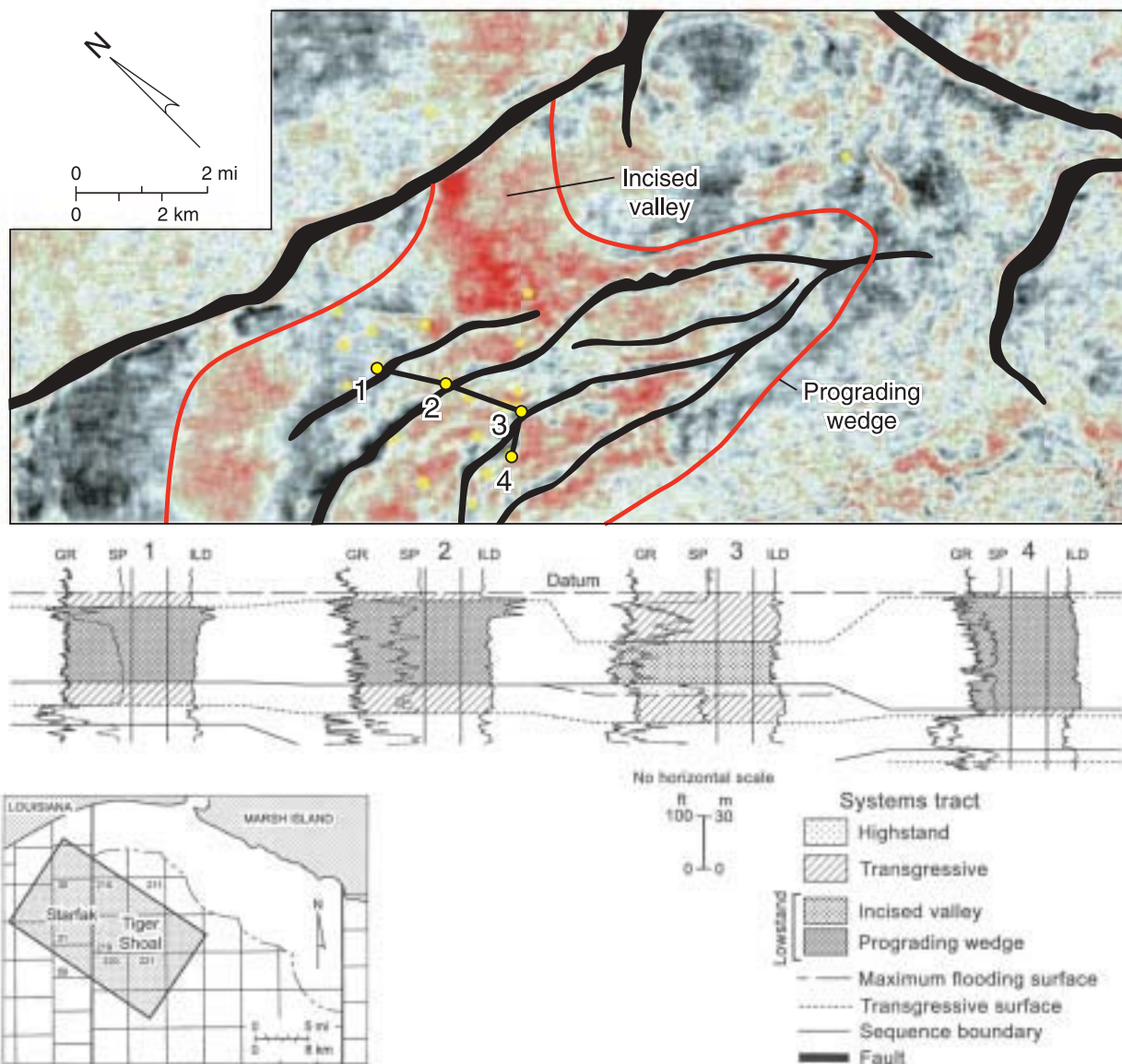


Figure 9. Amplitude stratal slice and well-log expression of the uppermost fourth-order prograding wedge in sequence 9 (Figure 8). Well 1 (Texaco No. 6, Vermilion Block 31, ~12,700–13,050 ft [~3871–3978 m]) captures the log expression of the margin of the wedge, whereas wells 2 and 4 (Texaco No. 8, Vermilion Block 31, ~12,700–13,000 ft [~3871–3962 m]), and Houston Oil & Minerals No. B-2(4), Vermilion Block 50, ~12,900–13,300 ft [~3932–4054 m]) exhibit the sandier accumulations within the central part. Well 3 (Houston Oil & Minerals No. E-1(9), Vermilion Block 50, ~12,850–13,200 ft [~3917–4023 m]) probably represents fluvial deposition within an incised valley (sharp-based blocky-serrate sandstone) concurrent with wedge progradation, followed by estuarine and bay-head delta (retrogradational middle part and upper progradational sandstone, respectively) deposition. Imaging of the distal parts of most wedges is limited by the southwestern boundary of the 3-D seismic data volume. Relief on the first-order growth fault just north of the wedge probably formed the exposed shelf edge below which relative sea level fell during lowstand deltaic deposition.

thick, shale-dominated retrogradational interval. The upper division, two to four fourth-order highstand systems tracts (locally incised by valley fills and interstratified with thin transgressive systems tracts) composing a progradational sequence set, forms the third-order highstand systems tract.

The third-order lowstand systems tracts in the lower two medial sequences 8 and 7 record the transition from upper-slope, proximal parts of fourth-order prograding wedges (down-dip) to the on-shelf parts of fourth-order highstand deposits locally incised by valley fills that are equivalent to the wedges (up-dip). This

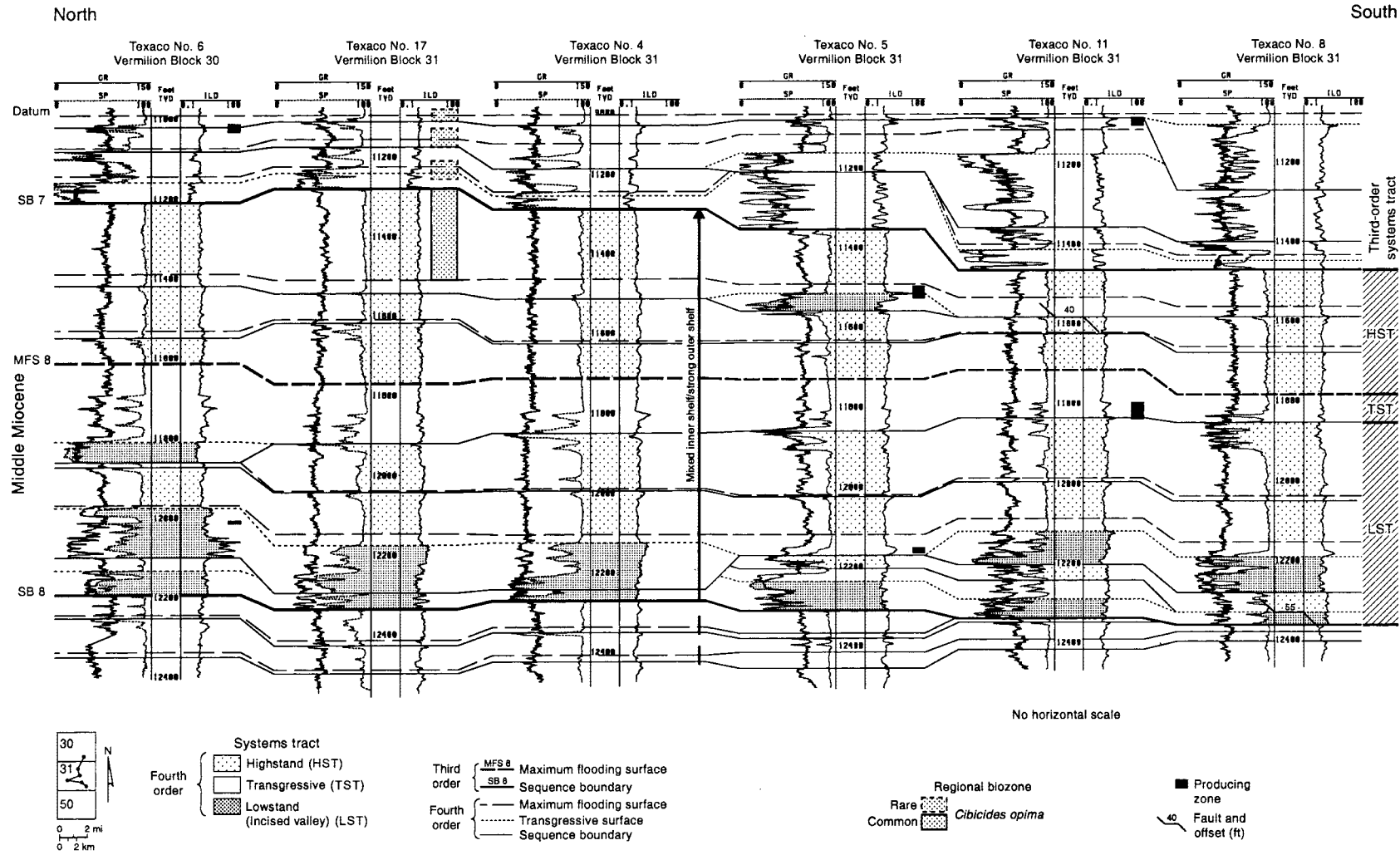


Figure 10. Dip cross section of medial third-order sequence 8 (middle Miocene), Starfak field. Fourth-order incised-valley systems in the third-order lowstand systems tract can be correlated to prograding wedges in wells downdip of, and lateral to, those shown in this cross section. Fourth-order incised-valley-fill, transgressive, and highstand deltaic/strandplain sandstones, mostly in the third-order lowstand systems tract, produce hydrocarbons. Biozone "boxes" record vertical variance for the top of each zone among the wells with fossil data. Paleobathymetric interpretations are based on benthic fossil assemblages: outer shelf = outer neritic and inner shelf = middle neritic to marginal marine (Table 1).

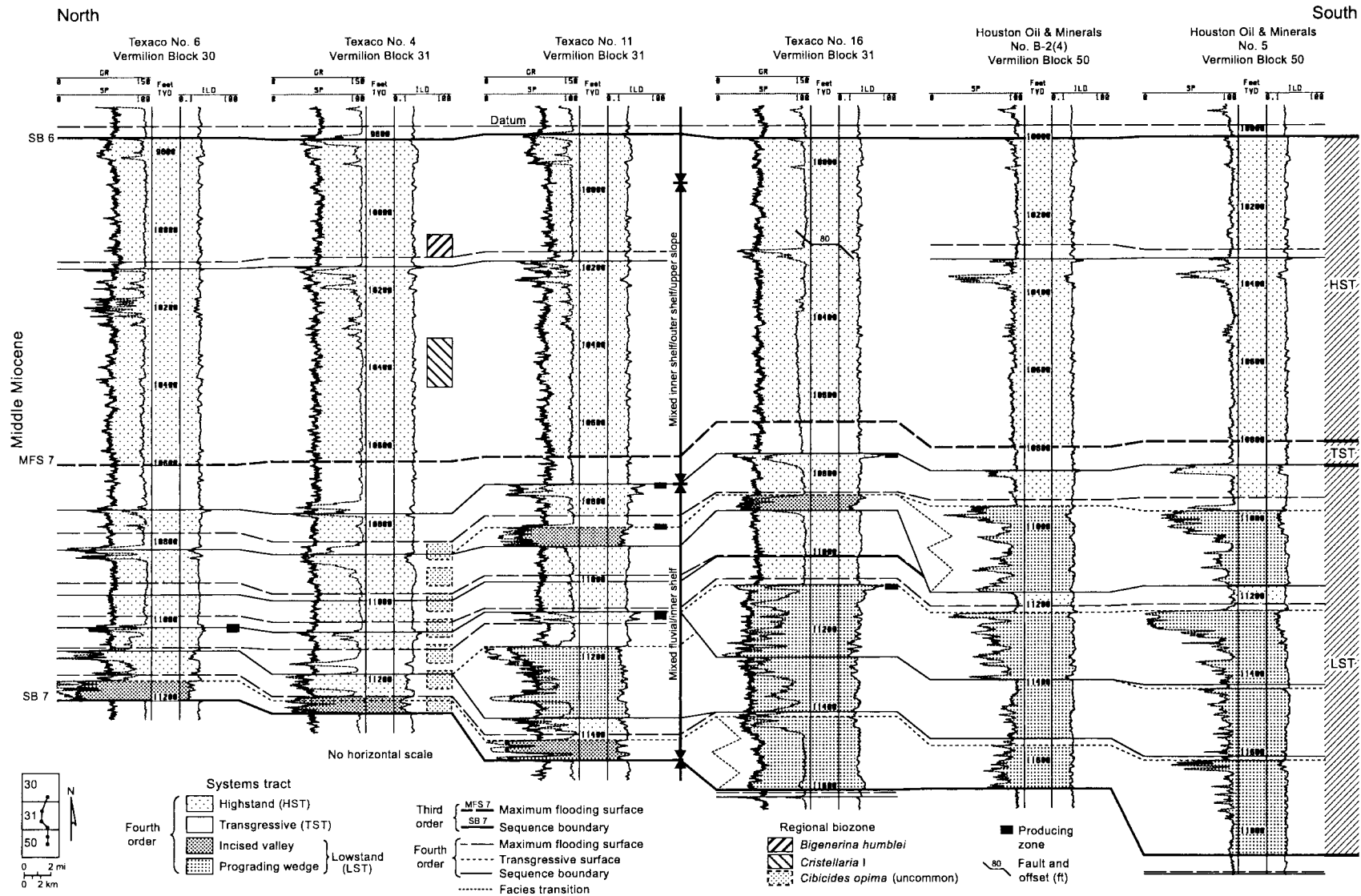


Figure 11. Dip cross section of medial third-order sequence 7 (middle Miocene), Starfak field. The third-order transgressive systems tract and basal highstand systems tract record the basinwide *Cristellaria l* transgression event. The lower fourth-order highstand systems tract of the third-order highstand deposits may contain additional fourth-order sequences. Fourth-order prograding-wedge, highstand deltaic/strandplain, and transgressive sandstones in the third-order lowstand systems tract compose the hydrocarbon reservoirs. Biozone "boxes" record vertical variance for the top of each zone among the wells with fossil data. Paleobathymetric interpretations are based on benthic fossil assemblages: upper slope = upper bathyal; outer shelf = outer neritic; and inner shelf = middle neritic to marginal marine (Table 1).

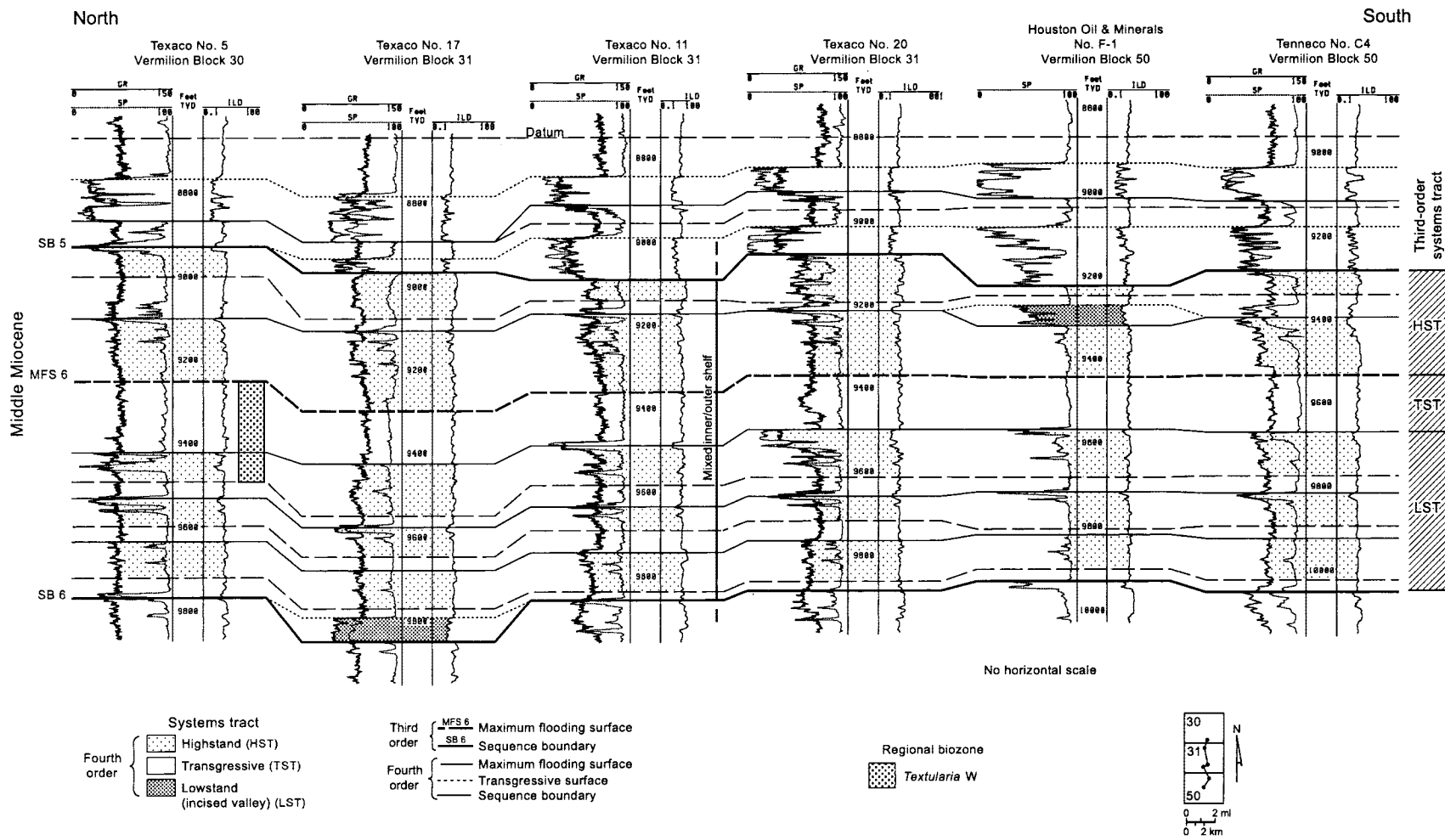


Figure 12. Dip cross section of medial third-order sequence 6 (middle Miocene), Starfak field. Biozone "box" records vertical variance for the top of the zone among the wells with fossil data. Paleobathymetric interpretations are based on benthic fossil assemblages: outer shelf = outer neritic and inner shelf = middle neritic to marginal marine (Table 1).

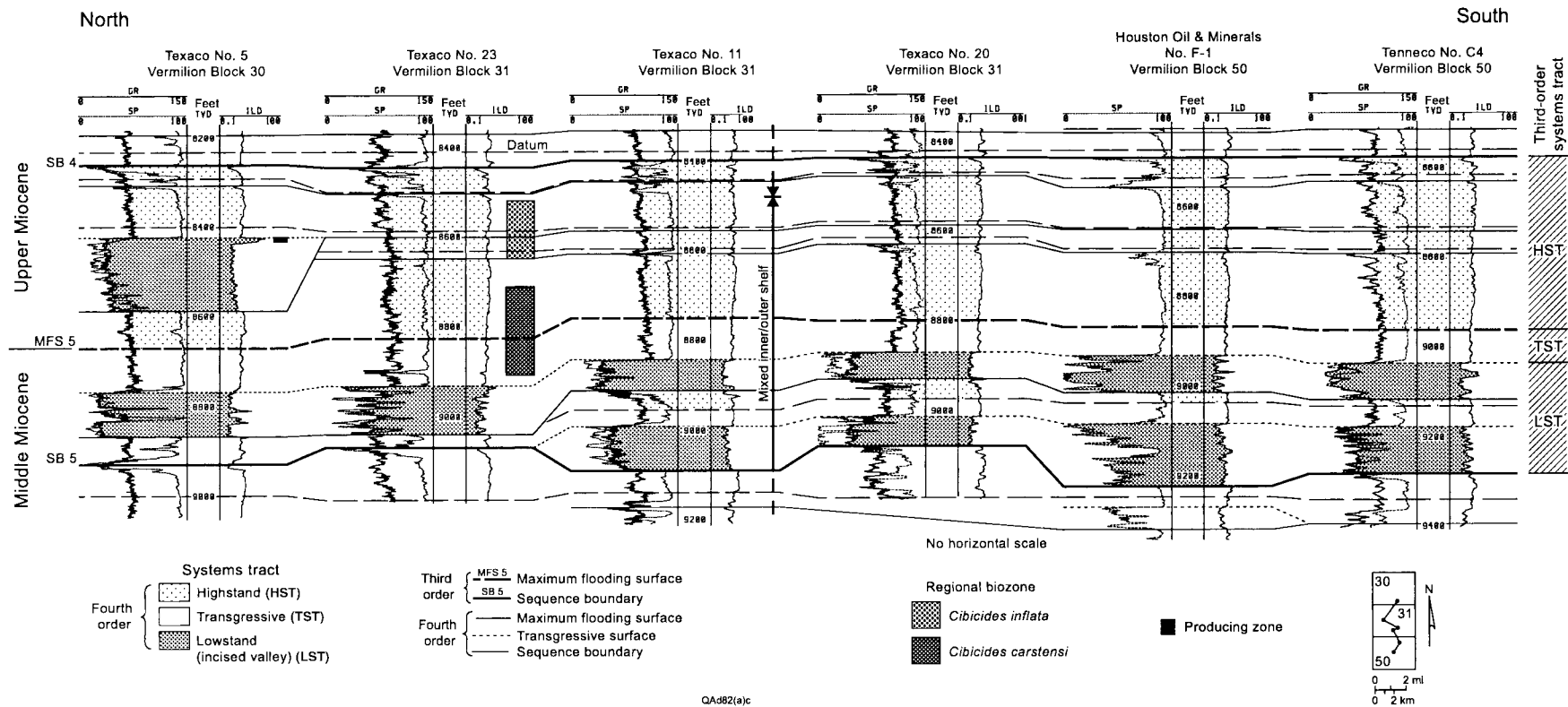
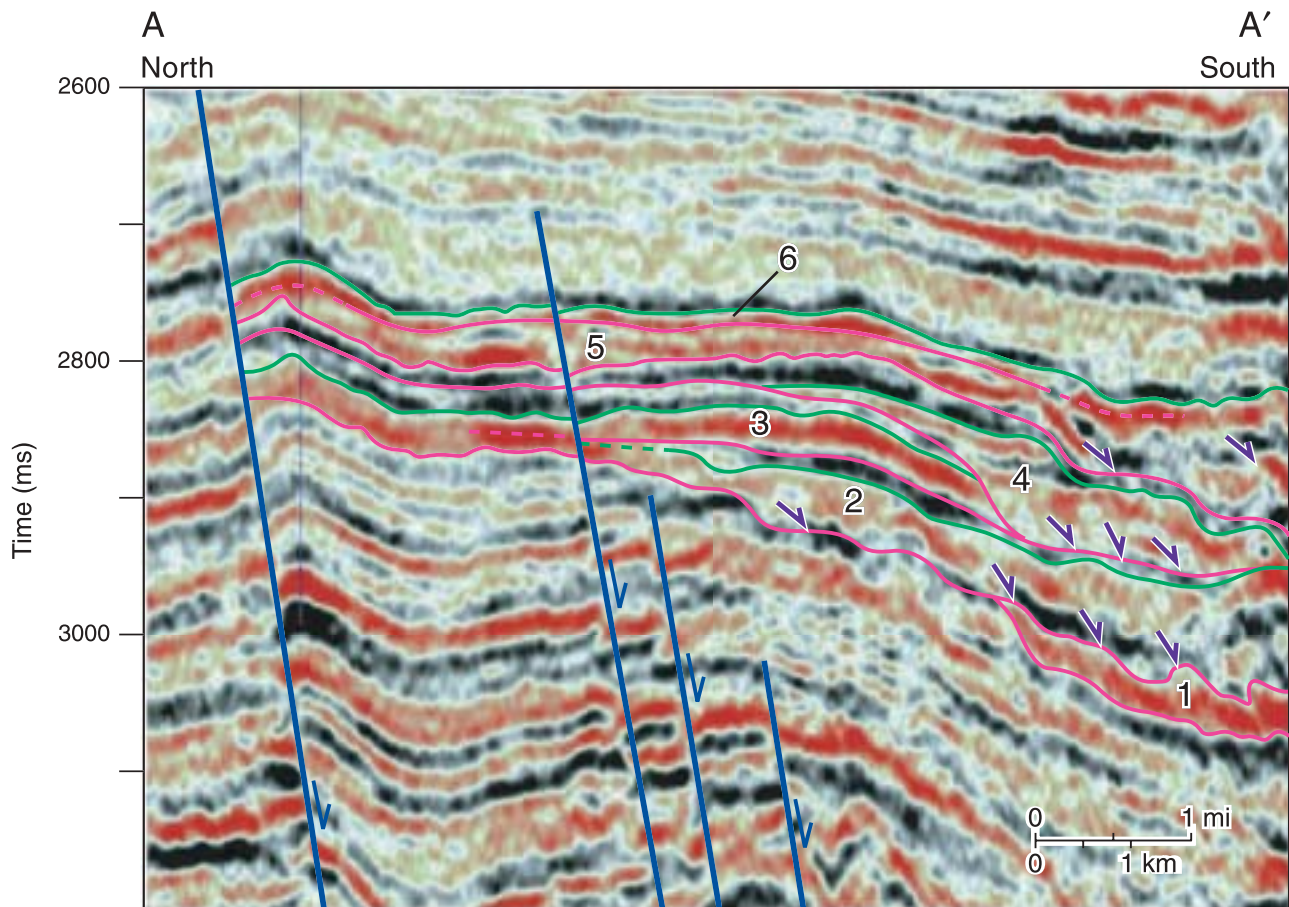
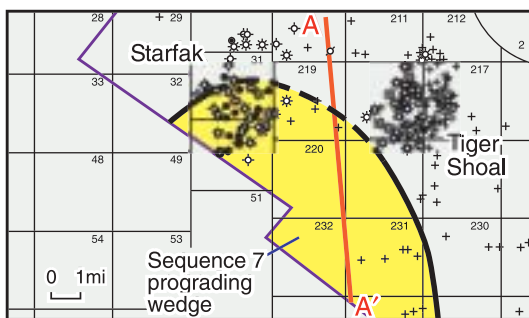


Figure 13. Dip cross section of medial third-order sequence 5 (middle and upper Miocene), Starfak field. The lower two incised valleys in the third-order lowstand systems tract are parts of the most extensive valley systems in the study area. Biozone “boxes” record vertical variance for the top of each zone among the wells with fossil data. Paleobathymetric interpretations are based on benthic fossil assemblages: outer shelf = outer neritic and inner shelf = middle neritic to marginal marine (Table 1).



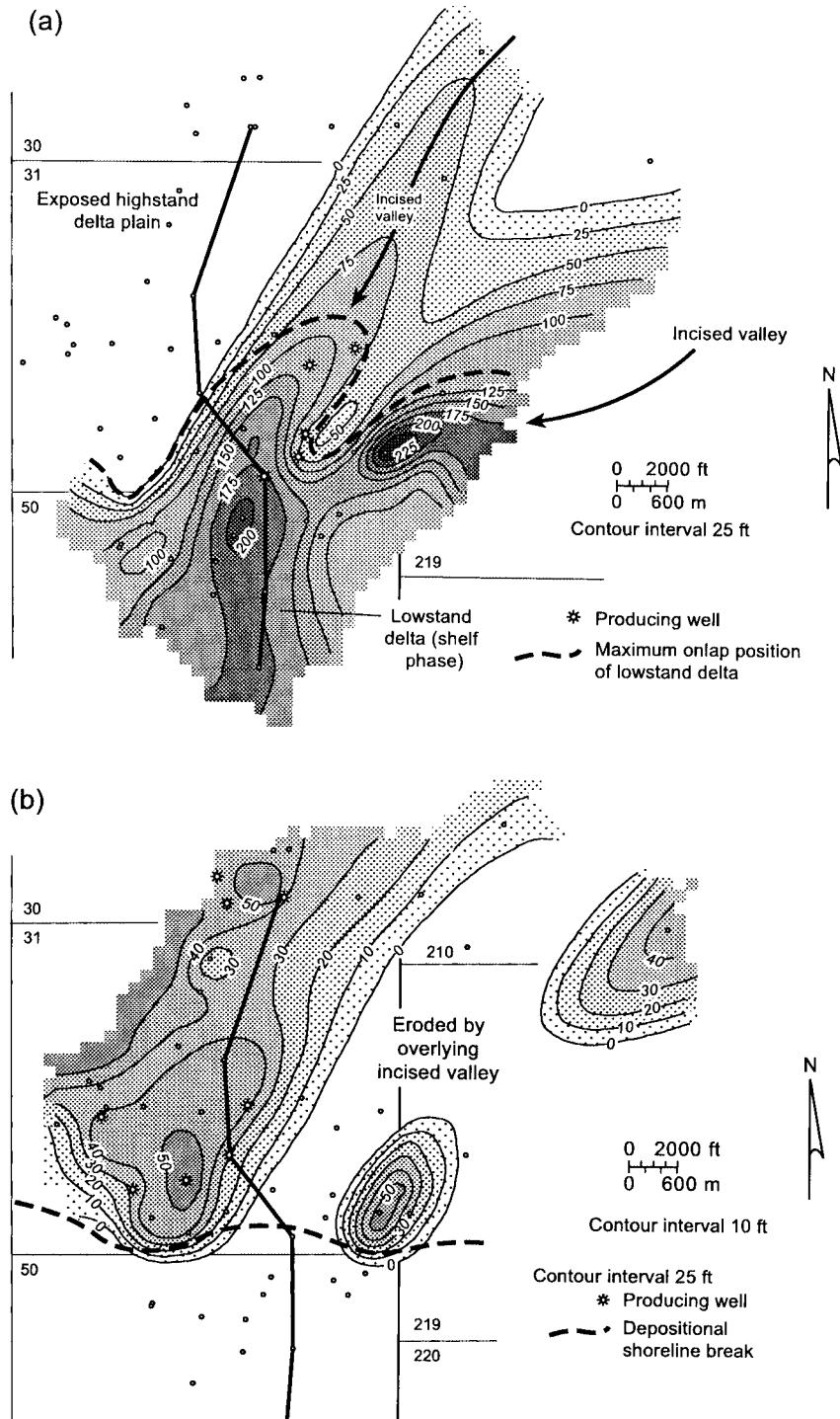
3 Seismic unit — Sequence boundary — Transgressive surface ↘ Downlap ⚡ Fault



A — A' Seismic profile — Perimeter of prograding complex
 - - - Fluvial sources — Perimeter of seismic survey

Figure 14. Depositional dip-oriented seismic profile of the third-order prograding wedge in sequence 7 (Figure 11). Seismic line depicts the wedge in an area near the southernmost limit of seismic coverage, therefore showing the most distal extent of the wedge that we can view. Seismic units 6, 5, and 4 correspond to the upper three fourth-order sequences defined in the area of well control. However, the seismic stratigraphy of seismic unit 3 is more complex; well-log correlation with the seismic indicates that unit 3 comprises the basal two fourth-order sequences in the area of well control. Seismic units 1 and 2 were deposited south and southeast of well control and represent coastally onlapping fourth-order prograding wedges. Third-order SB 7 at the base of the wedge was a major sediment-bypass surface across which the sediments in seismic units 1 and 2 were transported.

Figure 15. (a) Isochore map of the incised-valley-to-prograding-wedge transition in the third fourth-order sequence from the bottom of third-order sequence 7 (Figure 11), middle Miocene, Starfak field. Only the most proximal part of the prograding wedge has been drilled. (b) Isochore map of the fourth-order highstand systems tract that directly underlies, and was partially incised by, the valley/wedge complex shown in (a). No direct evidence of fault control of a shelf break is present, in contrast to the structural control on sequence 9's wedge deposition (Figure 9). Instead, this shelf-phase lowstand delta formed basinward of the depositional-shoreline break of the underlying highstand delta platform. Line of section is that of Figure 11. Both systems tracts contain productive sandstones. Petrophysical and engineering analysis suggests that sandstones of the two systems tracts form separate reservoir compartments.



transition is captured in sequences 7 (Figures 11, 14) and 8, although it is present in sequence 8 in wells downdip of, and lateral to, those shown in Figure 10. These third-order proximal prograding complexes represent a continuation of the overall upsection offlapping trend beginning with the distalmost lowstand deposits of sequence 10.

In the third-order lowstand systems tracts and much less commonly in the third-order highstand systems tracts, fourth-order blocky, blocky-serrate, and upward-fining sandstone units record lowstand incised-valley-fill aggradation. They are thickest (as much as ~250 ft [~76 m]) at the valley-to-wedge transition (Figure 15a), locally incising most or all of the under-

lying highstand systems tract (Figure 15b). In this transitional zone, the log facies of fourth-order incised-valley sandstones locally depict an aggradational pattern at the base of the unit and a progradational log trend at the top (e.g., at ~11,200 ft [~3413 m] in Texaco No. 16 [Figure 11] and Figure 9, well 3). These log characteristics suggest fluvial deposition within an incised valley concurrent with wedge progradation in this transitional zone, followed by deposition of a sandy bayhead delta during the subsequent transgressive phase. Because of the general difficulty of systematically correlating inferred thin bayhead-delta deposits within individual valley fills, we did not attempt precise correlation of these facies to differentiate true lowstand strata from overlying transgressive sediments in valley fills. However, these upper progradational sandstone units occur within correlated valley fills in updip wells, supporting inferred bayhead-delta deposition of the transgressive systems tract. Valley-fill channels (~40–250 ft [~12–76 m] thick) range between <0.5 and >5 mi (0.8 and 8 km, respectively) in width; one or both margins of the largest valleys cannot be resolved in our seismic volume, and maximum widths therefore cannot be measured. Incised valleys that we have mapped (Figure 16) and/or resolved seismically within the 352-mi² (912

km²) study area (Figure 17) commonly compose complex valley-axis systems that are probably widespread along exposure surfaces (sequence boundaries) across the Miocene shelf at the Central Mississippi and East Mississippi sediment-dispersal axes (sensu Galloway et al., 2000). This point is supported by Van Wagoner et al. (1990, their figures 22 and 23), who correlated and mapped the distribution of an incised-valley system (as much as 240 ft [73 m] thick), which is equivalent to, and updip (~90 mi [~145 km] northeast) of, a fourth-order valley system near the base of our middle Miocene sequence 7. Within an area of approximately 1900 mi² (~4921 km²; about five times the size of our seismic area), they resolved a valley system that attains a maximum width of more than 40 mi (64 km) and displays a complexity of merging valley axes comparable to that in our study area.

The areal dimensions of fourth-order highstand deltas of the medial and proximal third-order sequences (Figure 18) contrast sharply with those of the more areally restricted depocenters of the lowstand deltas (Figure 9). Whereas the perimeters of some lowstand deltas can be seismically resolved in the 352-mi² study area, the geographic expanse of highstand deltas of third-order lowstand and high-

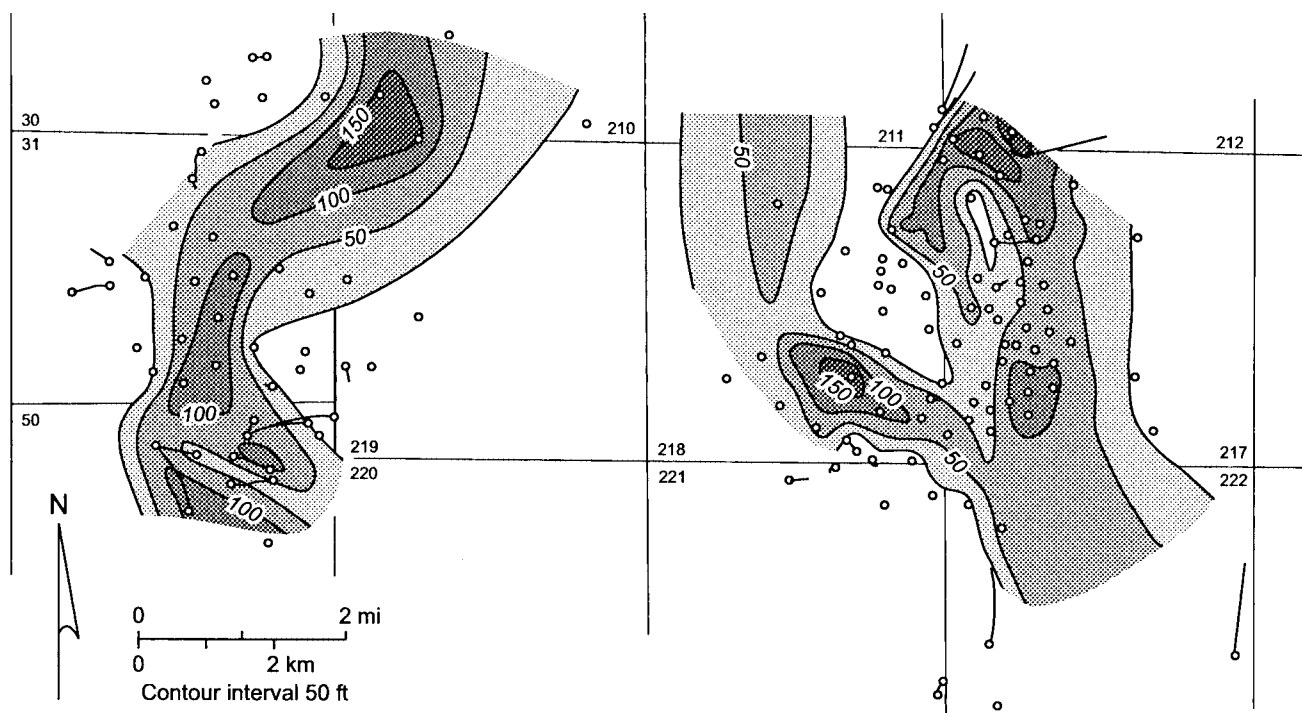


Figure 16. Isochore map of the incised-valley system at the base of third-order sequence 5 (Figure 13), middle Miocene, Starfak (west) and Tiger Shoal (east) fields. Fault-controlled structural highs in Tiger Shoal field that currently contribute to hydrocarbon trapping also locally influenced the direction of channel pathways during incision and valley-fill aggradation.

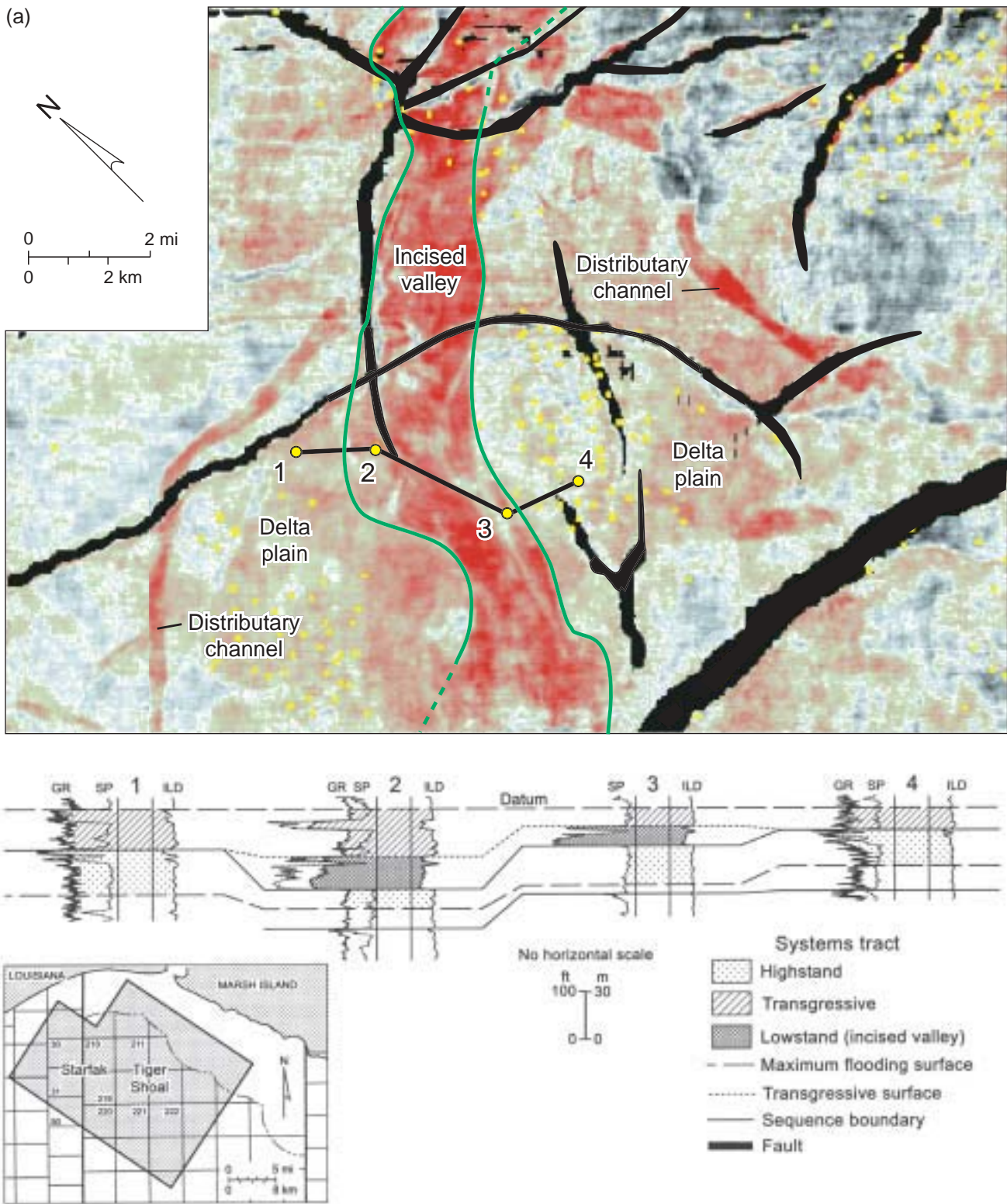


Figure 17. Representative amplitude stratal slices of lowstand incised-valley fills characteristic of the third-order medial and proximal sequences. (a) Amplitude stratal slice and well-log expression of a valley fill incising highstand delta-plain deposits (lower part of third-order highstand systems tract, sequence 4 [Figure 19]). Well 1 = British Borneo No. 176, South Marsh Island Block 210, ~7950–8200 ft (~2423–2499 m); well 2 = Texaco No. 95, South Marsh Island Block 210, ~7800–8150 ft (~2377–2484 m); well 3 = Texaco No. 54, South Marsh Island Block 218, ~7900–8150 ft (~2408–2484 m); and well 4 = Texaco No. 83, South Marsh Island Block 218, ~7800–8050 ft (~2377–2454 m).

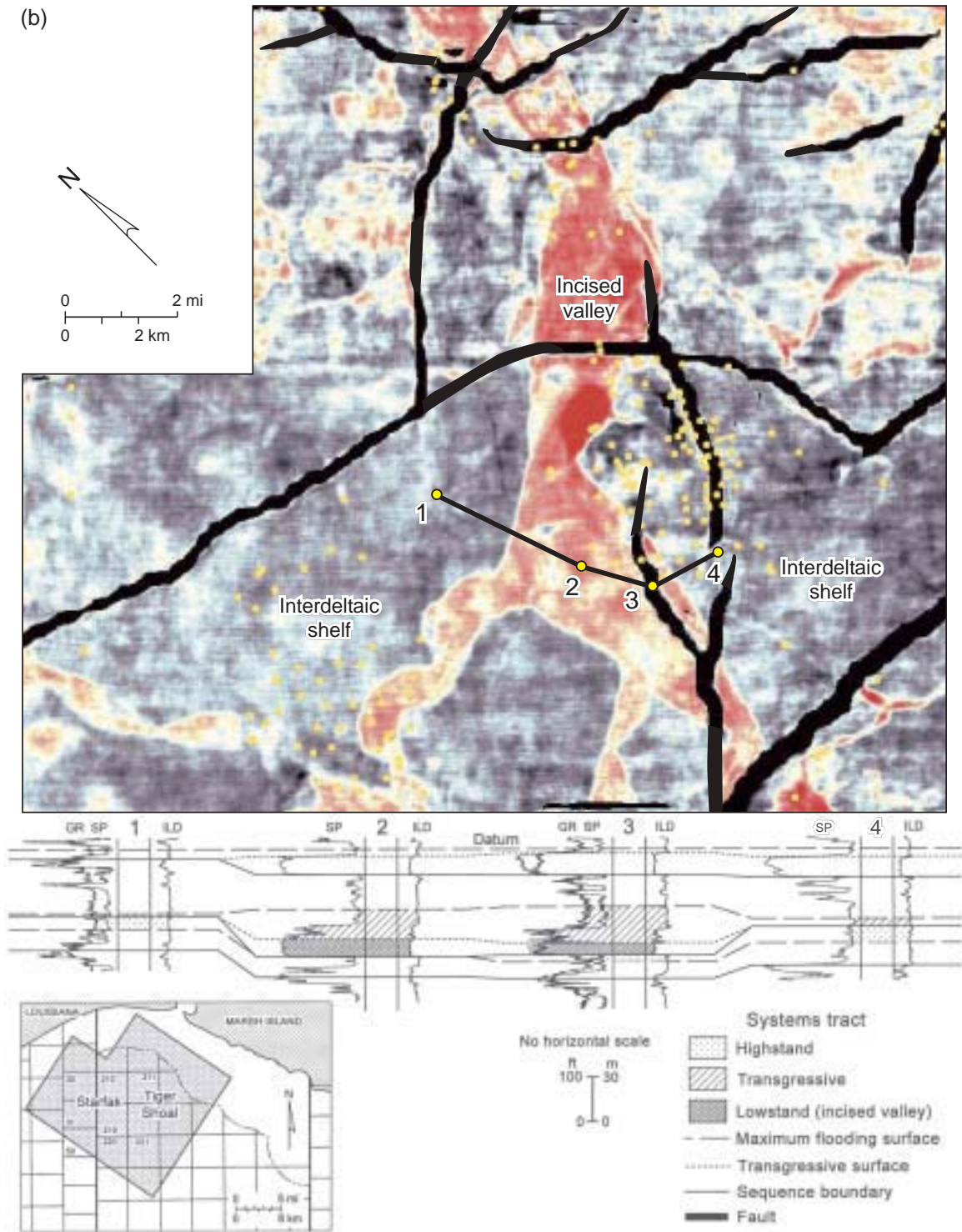


Figure 17. Continued. (b) Stratal slice and well-log expression of a valley fill incising interdeltaic deposits (upper part of third-order lowstand systems tract, sequence 2 [Figure 21]). Note well-developed delta-plain sandstones below SB (exposure surface) equivalent to that below the valley fills (unconformity) in wells 1 and 4 of (a), in contrast to the shaly interdeltaic deposits below the exposure surface in wells 1 and 4 in (b). Well 1 = Texaco No. 95, South Marsh Island Block 210, ~6900–7200 ft (~2103–2195 m); well 2 = Texaco No. 54, South Marsh Island Block 218, ~6850–7200 ft (~2088–2195 m); well 3 = Texaco No. 99, South Marsh Island Block 221, ~7050–7400 ft (~2149–2256 m); and well 4 = Texaco No. 77, South Marsh Island Block 221, ~6800–7100 ft (~2073–2164 m).

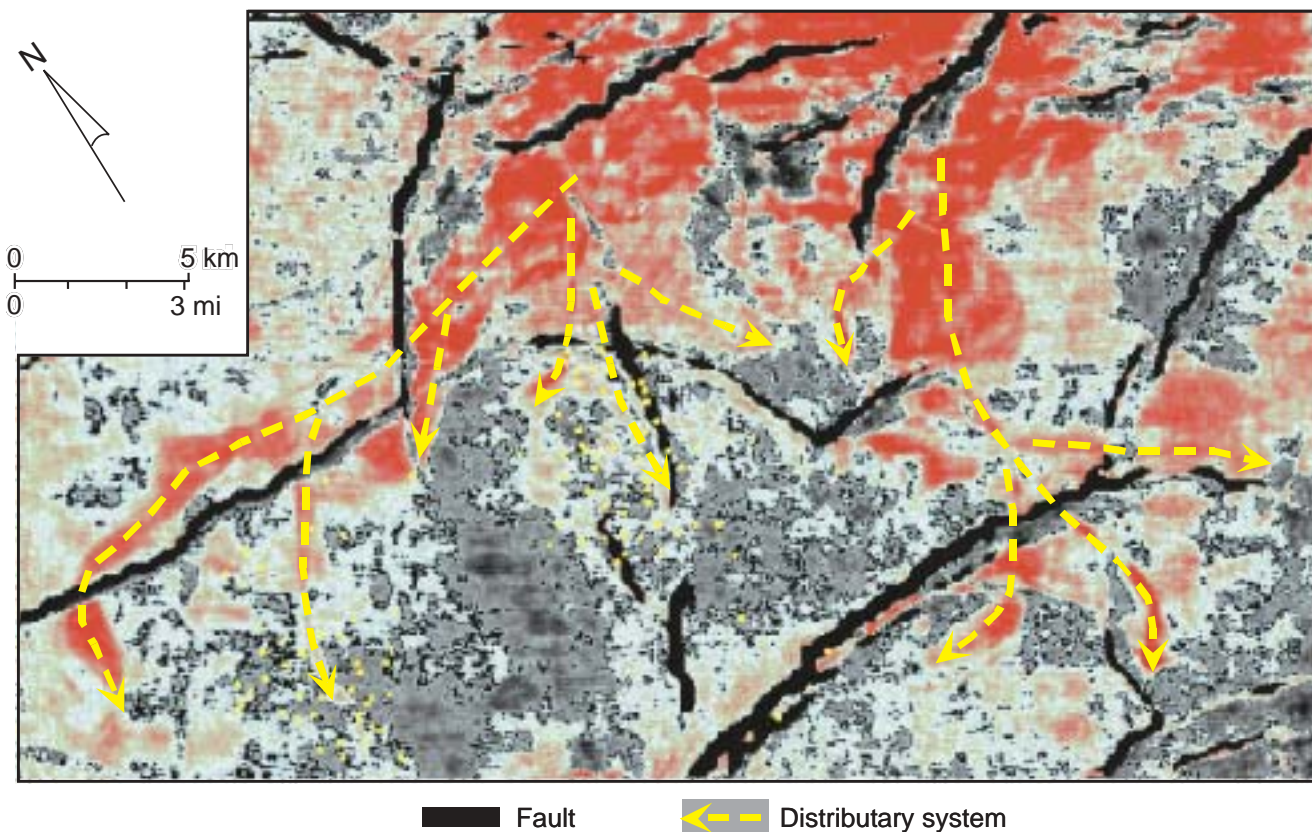


Figure 18. Representative amplitude stratal slice of part of a digitate highstand delta system (upper part of third-order highstand systems tract, sequence 4 [Figure 19]) characteristic of the third-order medial and proximal sequences. Note probable syndepositional fault control of the western distributary system. Area coincides with that of the seismic surveys shown in Figure 1.

stand systems tracts greatly exceeds that of our study area. Typically, only one or two distributary lobes of a highstand delta can be resolved in stratal slices (Figure 18), and only part of a single lobe occurs in maps of the areas of well control. The smaller areal dimensions of the lowstand deltas are consistent with more focused sedimentation via the funneling effect of feeder incised valleys (Posamentier and Vail, 1988).

The third-order transgressive systems tracts in the medial sequences are thicker and more easily resolved on well logs than those of the distal sequences. In depositional-dip profile, the third-order transgressive systems tracts decrease in thickness and contain fewer progradational sandstones (of very thin fourth-order systems tracts) distally over a distance of 2–4 mi (3–6 km; best shown in Figure 10), reflecting retrogradation and increasing distance from sediment-source areas. Four of the five third-order MFSs in the medial sequences coincide with major faunal floods (Figure 5) recorded in the associated marine condensed sections. The exception, the MFS of sequence 8, occurs at the base of a broad faunal peak.

The fourth-order sequences that compose the third-order transgressive systems tracts in our 10 sequences are generally very thin (≤ 35 ft [11 m]), shaly, and difficult to correlate regionally. Therefore, we did not delineate these high-frequency sequences within the third-order transgressive systems tracts on our cross sections. However, the retrogradational pattern of the higher order, sandstone-bearing sequences is quite evident in depositional-dip-oriented cross sections that transect presumed sand depocenters (e.g., Figure 10).

Proximal Sequences (SB 4 to SB 0)

Stratal Characteristics

Proximal third-order sequences 4 through 1 (upper Miocene, SB 4 to SB 0) extend from approximately 75 ft (~ 23 m) above the *Cibicides inflata* regional biozone to approximately 150 ft (~ 46 m) above the *Bigenerina* A biozone (Figures 19–22). These proximal sequences are the thinnest of all 10 third-order sequences, ranging between approximately 375 and 700 ft (~ 114 and 213 m) respectively, in thickness. Like the medial

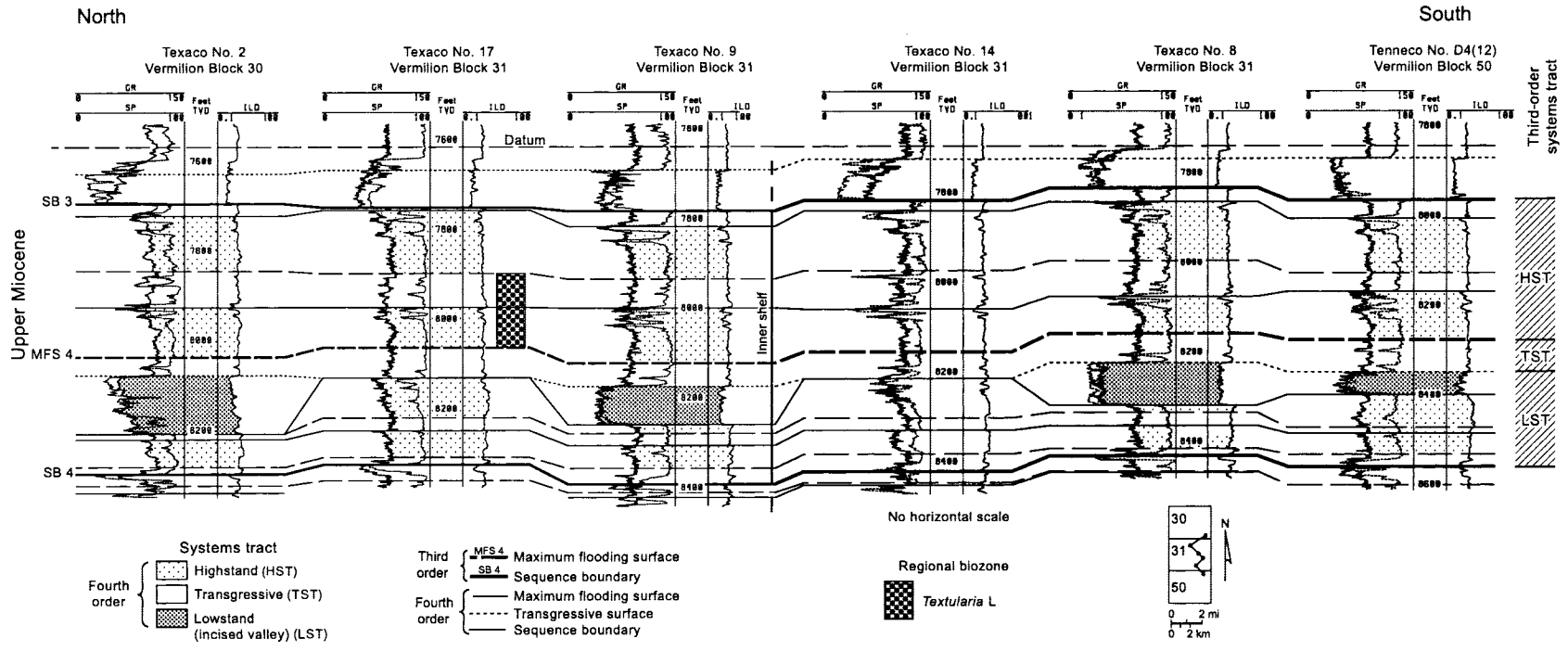


Figure 19. Dip cross section of proximal third-order sequence 4 (upper Miocene), Starfak field. Biozone "box" records vertical variance for the top of the zone among the wells with fossil data. Paleobathymetric interpretations are based on benthic fossil assemblages: inner shelf = middle neritic to marginal marine (Table 1).

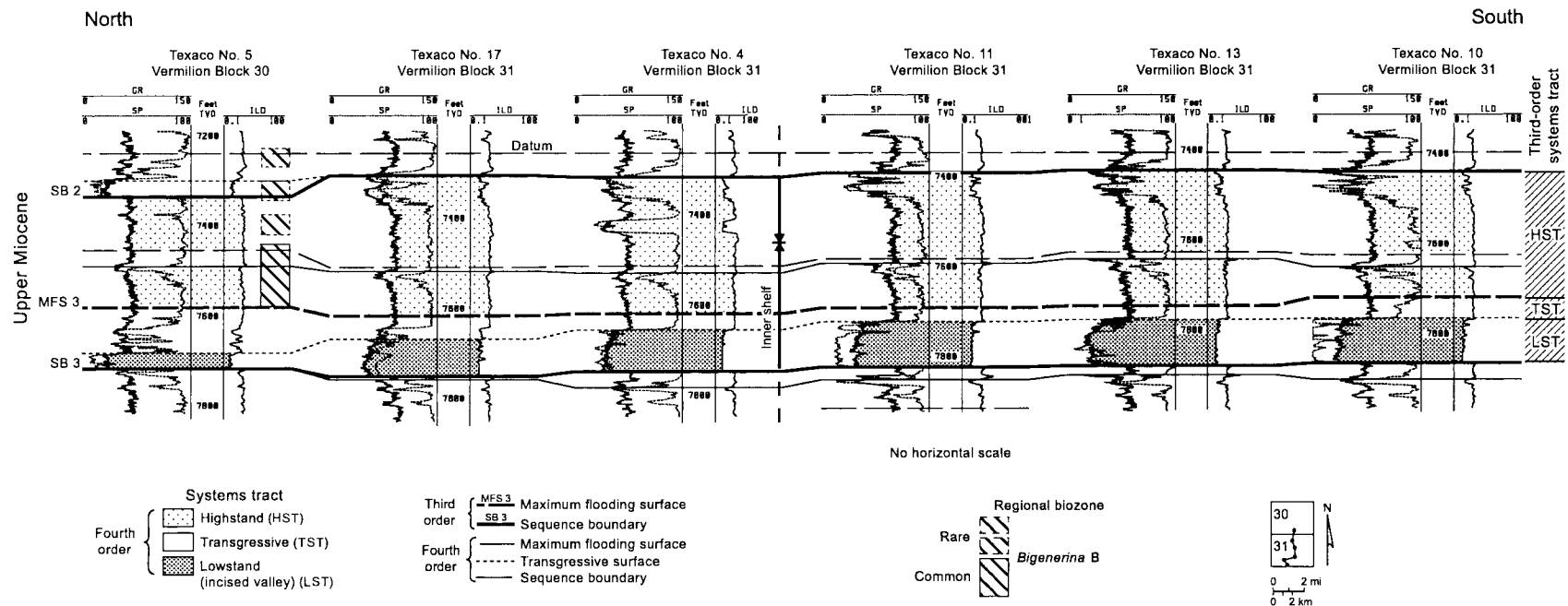


Figure 20. Dip cross section of proximal third-order sequence 3 (upper Miocene), Starfak field. Biozone “boxes” record vertical variance for the top of each zone among the wells with fossil data. Paleobathymetric interpretations are based on benthic fossil assemblages: inner shelf = middle neritic to marginal marine (Table 1).

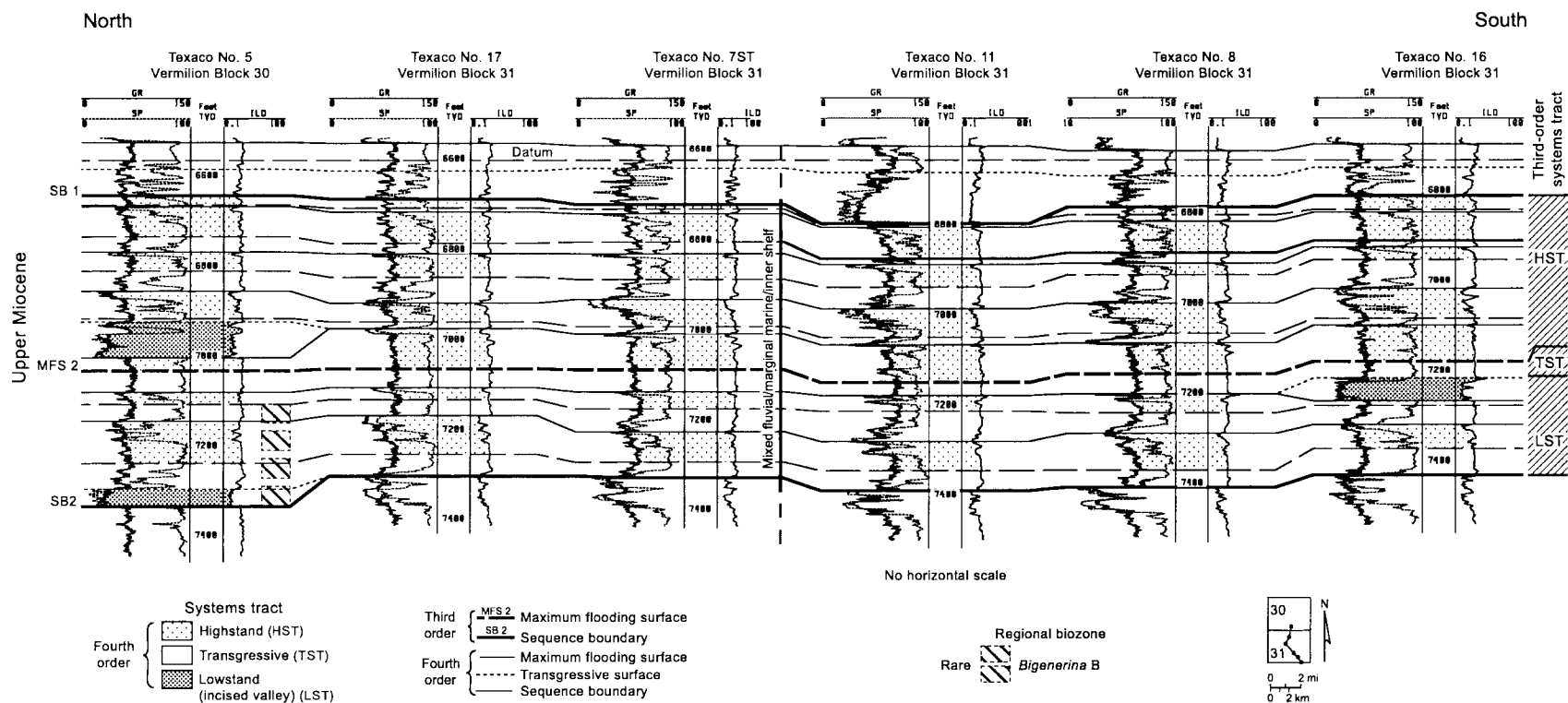


Figure 21. Dip cross section of proximal third-order sequence 2 (upper Miocene), Starfak field. Biozone “boxes” record vertical variance for the top of each zone among the wells with fossil data. Paleobathymetric interpretations are based on benthic fossil assemblages: inner shelf = middle neritic to marginal marine (Table 1).

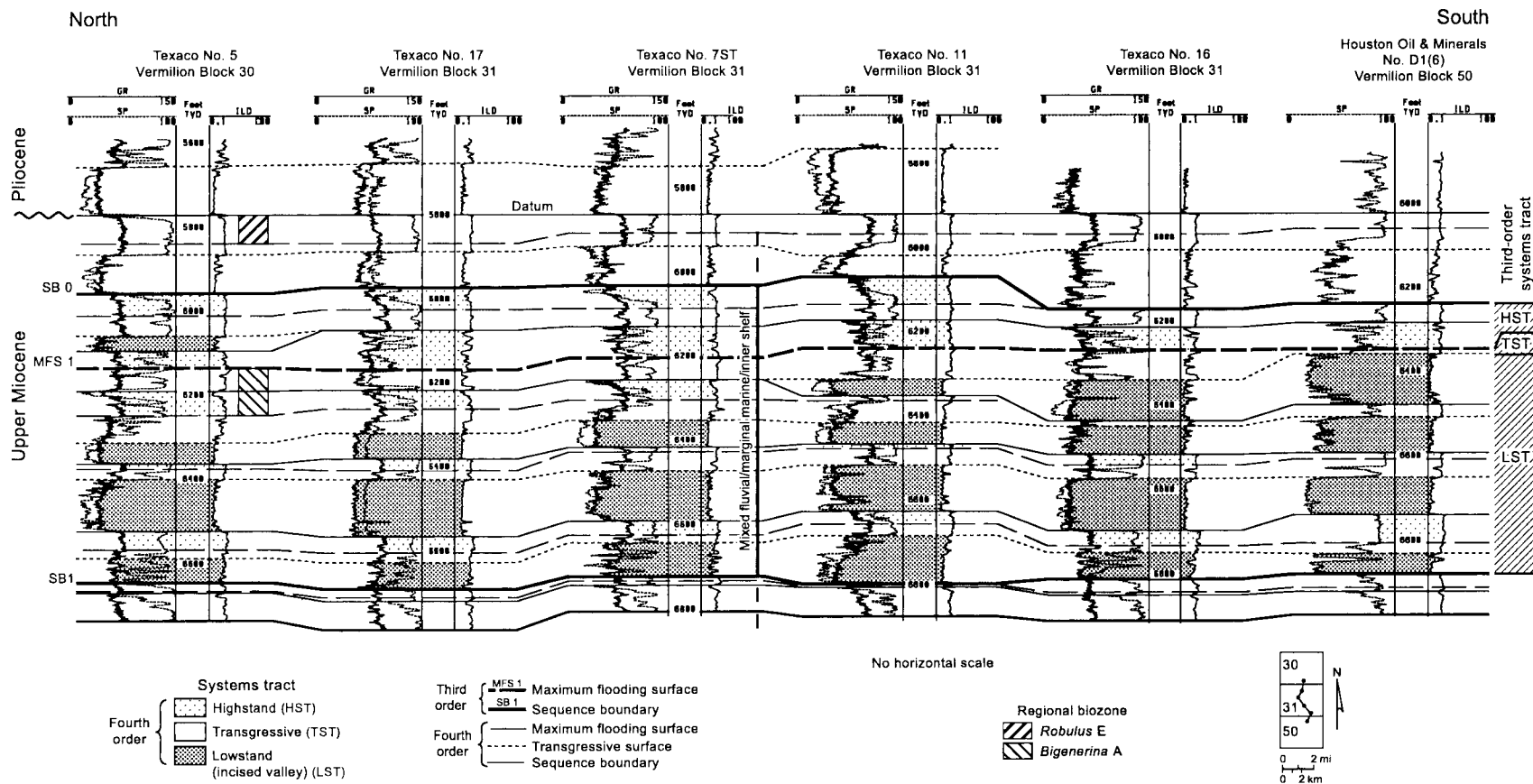


Figure 22. Dip cross section of proximal third-order sequence 1 (upper Miocene), Starfak field. Biozone “boxes” record vertical variance for the top of each zone among the wells with fossil data. Paleobathymetric interpretations are based on benthic fossil assemblages: inner shelf = middle neritic to marginal marine (Table 1).

sequences, each of the proximal sequences comprises three stratigraphic divisions: (1) a lower succession of one to three aggradational (~40–130 ft [~12–40 m] thick) or progradational (~25–80 ft [~8–24 m] thick) units; (2) a locally thick (~35–70 ft [~11–21 m]), upward-fining, retrogradational, shale-dominated section in the middle; and (3) an upper section of typically two to five (~30–200 ft [~9–61 m] thick) mostly progradational units of thicker shales and sandstones. Progradational and aggradational units in the lower and upper divisions are interstratified with thinner (~10–70 ft [~3–21 m]) retrogradational intervals. However, the proximal sequences are differentiated from the medial ones by having a higher proportion of blocky and blocky-serrate aggradational sandstones and thinner progradational units that contain a higher percentage of sandstone. The retrogradational units in the lower and upper divisions also contain a higher percentage of sandstone than those in the medial sequences but are of comparable thickness.

Systems Tracts

The lower, middle, and upper stratigraphic divisions of the proximal sequences represent third-order lowstand, transgressive, and highstand systems tracts, respectively. These systems tracts accumulated in water environments shallower than those of the medial sequences: inner-shelf to fluvial settings in marine water depths that ranged from middle neritic to marginal marine, as indicated by fossil data (Figures 4, 19–22). One to three relatively thin (~75–130 ft [~23–40 m]) closely spaced fourth-order sequences form the third-order lowstand systems tract. The third-order lowstand systems tract is overlain by the third-order transgressive systems tract. The upper division, two to five fourth-order highstand systems tracts (locally incised by valley fills and interstratified with thin transgressive systems tracts) composing a progradational sequence set, forms the third-order highstand systems tract. The more abundant valley-fill sandstone units commonly incise the separate progradational and retrogradational units that best define the cyclic stratal patterns within the third-order sequences, making the defining of these proximal third-order sequences more challenging, especially in sequence 1 (Figure 22).

In the area of well-log control and within the area of seismic coverage, the proximal sequences show minimal variation in overall thickness or stratal-stacking patterns (“railroad tracks” on seismic profiles). No lowstand prograding complexes can be resolved either on seismic or well logs in the downdip parts of the

study area. In the lower Pliocene succession above sequence 1, incised-valley sandstones compose an upward-increasing percentage of the section, grading to stacked fluvial channel fills, and thin and volumetrically minor overbank and marine-flood shales in a dominantly coastal-plain setting (Zeng et al., 2001a). Third-order MFSs generally coincide with regional faunal-abundance peaks (Figure 5).

Correlation with Eustatic Cyclicity

Although biostratigraphic data show that the absolute ages of our third-order sequence boundaries approximately coincide with those defined by Haq et al. (1988), updated with the revised chronology of Berggren et al. (1995), the third-order cyclicity interpreted in our study differs from that represented in Haq’s generalized (global) coastal-onlap curve (Figure 23). Whereas the Haq curve shows transgressive trends in the upper lower to lower middle Miocene and throughout the upper Miocene, we observe prominent regressive signatures in the study area during these periods. In fact, our entire study interval is a regressive succession at the third-order scale. The study area lies within the Miocene Central Mississippi sediment-dispersal axis (Galloway et al., 2000). Therefore, the difference between the “average” global pattern and that of offshore Louisiana is best explained by the basin-specific effects of generally high sediment flux throughout the Miocene in the vicinity of the ancestral Mississippi delta.

In contrast to the global third-order sequences of Haq et al. (1988), we identified three third-order cycles between 11.70 and 9.26 Ma a time interval of 2.44 m.y. that Haq et al. (1988) identified as representing one third-order cycle (Figure 23). Styzen (1996) also concluded that there are multiple cycles within this time range, although he did not differentiate between third- and fourth-order sequences. However, the duration of one of his four cycles (~0.9 m.y.) within this time range is comparable to the duration of Haq’s shorter term Miocene third-order sequences (0.9 m.y.), using the updated chronology of Berggren et al. (1995). Therefore, Styzen’s cycle boundaries of the 11.70- to 9.26-Ma period probably record at least two third-order sequences.

Our inferred coastal-onlap trend for most of the Miocene of offshore Louisiana more closely coincides with observations presented by Hardenbol et al. (1998) for Miocene strata in European basins. In the same time interval, they differentiated parts, or all, of three

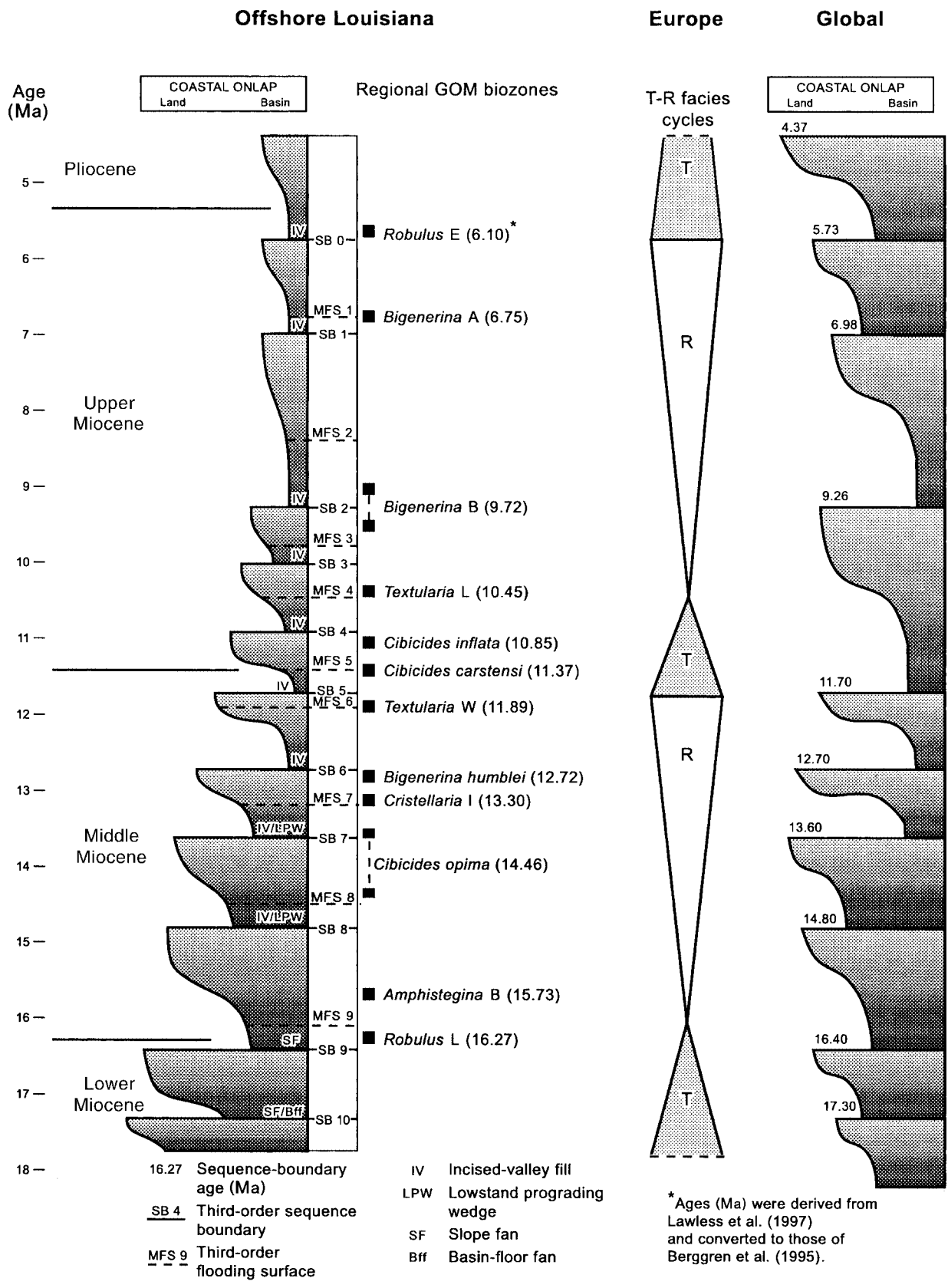
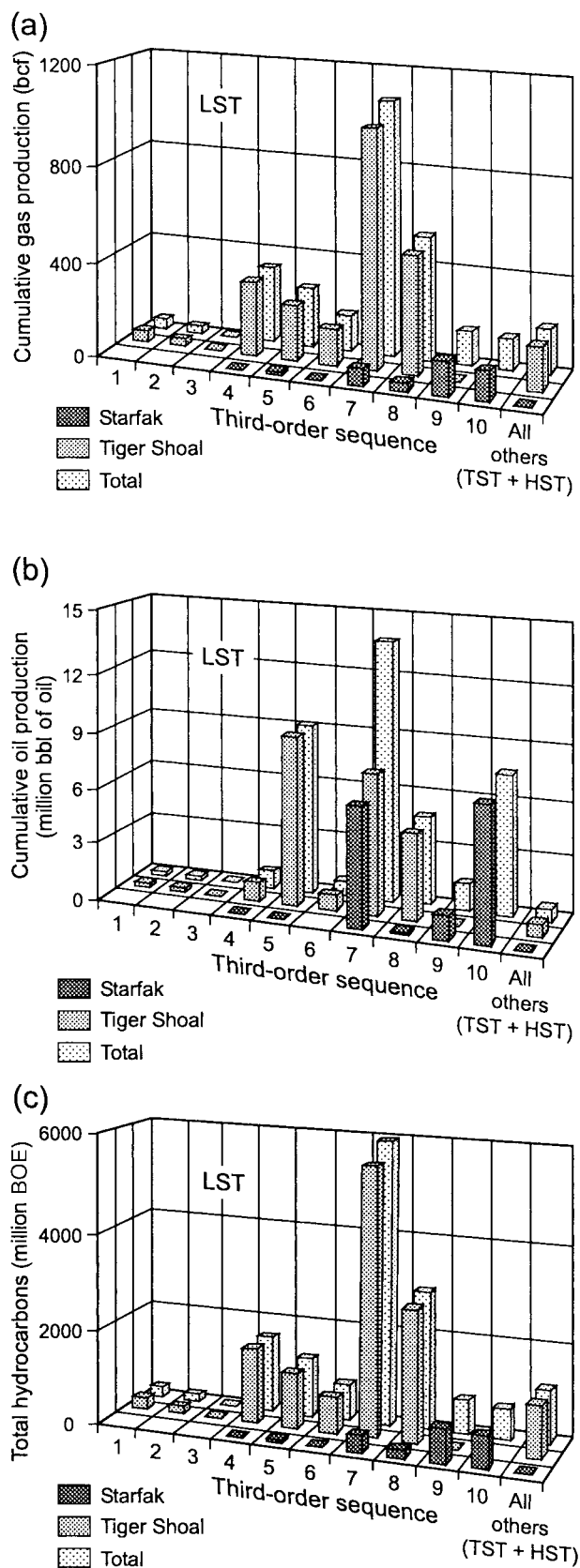


Figure 23. Comparison of the coastal-onlap curve of the study area (offshore Louisiana), the T-R cycles of Hardenbol et al. (1998) for European basins, and the global curve of Haq et al. (1988). GOM = Gulf of Mexico.



low-order transgressive-regressive (T-R) facies cycles (Figure 23), which coincide with third-order sequence sets. As in our study interval, long-duration regressive periods dominate. However, unlike offshore Louisiana, the European Miocene regressive succession is punctuated by relatively short-lived but significant (second-order?) transgressive events. The differences among these three cycle schemes probably lie in basin-specific variations in the interaction of eustasy, sediment supply, and subsidence, which control stacking trends of third-order sequences (Hardenbol et al., 1998).

RELATION OF PRODUCTION TO SYSTEMS TRACTS

Within individual fourth-order systems tracts of Starfak and Tiger Shoal fields, hydrocarbons have been produced from inferred lowstand incised-valley fills, deltaic/strandplain sandstones of late highstand systems tracts, deltaic sandstones of late lowstand prograding wedges, and transgressive bayhead deltaic sandstones. However, calculation of the vertical distribution of production in Starfak and Tiger Shoal fields indicates that the vast majority of gas and oil production is from the third-order lowstand systems tracts at the bases of the third-order cycles (Figure 24).

Within Starfak and Tiger Shoal fields, reserves are concentrated where fourth-order systems tracts stack to form third-order lowstand systems tracts, which compose approximately 30–50% of the total study interval. Production records through July 1, 2000, indicate that 92.6% of all gas production, 98.0% of all oil production, and 92.6% of total hydrocarbon production have come from lowstand systems tracts of the third-order sequences. The third-order lowstand systems tract of sequence 7 (Figure 11) has produced the majority of total hydrocarbons, followed by the lowstand deposits of sequence 8 (Figure 10). However,

Figure 24. Bar graphs of cumulative hydrocarbon production (through July 1, 2000) from the 10 third-order lowstand systems tracts in Starfak and Tiger Shoal fields. The category "All others" represents cumulative production from all third-order highstand and transgressive systems tract reservoirs. (a) Cumulative gas, (b) cumulative oil, and (c) total hydrocarbons. Cumulative production from Starfak is approximately 357.2 bcf gas, 15.0 million bbl of oil, and 2.0 billion BOE total hydrocarbons. Totals for Tiger Shoal are 2.4 tcf gas, 24.1 million bbl of oil, and 13.5 billion BOE total hydrocarbons.

the prograding-wedge sandstones of sequence 10 (Figure 7), which are deep targets, have only recently been developed and are currently primary prospect targets. Although a dominant structural-trapping component is present in the fields (DeAngelo and Wood, 2001), most of the resource distribution can be predicted by understanding its context within a framework of key sequence-stratigraphic surfaces. These key surfaces have a strong control on hydrocarbon distribution.

Hydrocarbons are dominantly distributed in third-order lowstand systems tracts because these intervals have optimal reservoir-quality and seal juxtapositions. Miocene shales of the northern Gulf of Mexico are generally believed not to be source rocks; the presumed primary source rocks for Miocene reservoirs of offshore Louisiana are shales of the Paleocene Midway, and Eocene Wilcox and Sparta formations (Nehring, 1991). Most reservoirs occur within the third-order lowstand systems tracts for several reasons, considered collectively:

- Prominent shales of the third-order slope fans and third-order transgressive and highstand systems tracts create thick regional hydrocarbon seals over reservoirs within the third-order lowstand systems tracts (e.g., Figures 7, 8 [slope fans], 11 [transgressive and highstand systems tracts]).
- These thick sealing shales above and below the productive zones minimize the risk of cross-fault juxtaposition of lowstand reservoir sandstones against third-order highstand sandstones that can act as points of leakage.
- The common juxtaposition of thick incised-valley sandstones against neritic to shallow-marine shales from lowstand incision (e.g., Figure 13, Texaco No. 5 well, valley fill incised into middle-neritic shales containing *Cibicides carstensi* [Table 1]) creates lateral and upper seals at valley margins (e.g., Bowen et al., 1993).
- The areally restricted distribution of commonly thick, stacked, deltaic-wedge sandstones within slope and basinal shales creates ideal conditions for potential hydrocarbon migration and stratigraphic entrapment.

Based on these observations and rationale, we think that there are significant untapped hydrocarbon accumulations in nonstructural traps within the study area. Moreover, hydrocarbon concentrations most likely occur in third-order systems tracts comprising both nonstructured and structured Miocene strata in adjacent

on-shelf regions of the northern Gulf of Mexico. This pattern of resource distribution keyed to third-order lowstand systems tracts serves as a guide for more regional resource development. Inspection of limited well-log data from surrounding Miocene shelf fields (Light House Point, Mound Point, and South Marsh Island Block 236 [Amber Complex]) indicates that our sequence-stratigraphic framework of the Miocene series can be tied to these areas (Figure 1). We expect that the framework can be readily applied to other surrounding offshore fields, especially if supported by sufficient well-log and paleontologic data to reinforce correlation confidence.

CONCLUSIONS

We have developed a high-resolution sequence-stratigraphic framework of most of the Miocene succession in the vicinity of Starfak and Tiger Shoal fields, offshore Louisiana (Vermilion and South Marsh Island areas). Well-log, paleontologic, and seismic data indicate that the approximately 10,000-ft (~3048-m) regressive study interval grades upward from distal-lowstand basin-floor, slope-fan, and prograding-complex facies; through the lateral transition from prograding complexes to lowstand, highstand, and transgressive on-shelf deposits; and into proximal sequences deposited in mostly nearshore environments. These facies compose systems tracts within 10 third-order sequences and at least 58 fourth-order sequences ranging in age from the late Burdigalian (~17.3 Ma) to the early Messinian (~6.1 Ma), a span of ~11.2 m.y. The details of this framework provide a basis for its extrapolation into the extensive shelf-bound Miocene play fairways surrounding the study area and into potentially productive, deeper lower Miocene strata. For example, amplitude stratal slices of intervals keyed to the framework can image depositional geomorphology, potential trap locations, and sandstone concentrations of reservoir-scale systems tracts outside the areas of well control. Biostratigraphic data provide critical constraints on absolute age of the key chronostratigraphic surfaces and sequences, enabling comparison with published eustatic curves. The chronology of third-order sequences generally coincides with that of the Haq curve. However, Miocene coastal-onlap patterns of third-order sequences of offshore Louisiana deviate with the global “average” patterns of Haq and the T-R cycles of European basins because of sediment-supply and subsidence variations in the Gulf Coast basin.

A full range of systems tracts and depositional facies occur in the Miocene interval, and hydrocarbons have been produced from sandstone reservoirs within all fourth-order systems tracts. However, reserves are highly concentrated where the reservoir-scale fourth-order systems tracts stack to form third-order lowstand systems tracts, which compose approximately 30–50% of the succession. Within the two fields, greater than 90% of all gas and oil has been produced from third-order lowstand systems tracts. Although a dominant structural-trapping component is present in the fields, the sequence-stratigraphic context of reservoirs is an important indicator of resource-distribution patterns. The differentiation of high-frequency sequences and systems tracts within the developmentally mature Miocene succession of the study area and the observation that hydrocarbons are vastly concentrated within the Miocene third-order lowstand systems tracts provide an impetus for development of new Miocene hydrocarbon reserves both within the study area and in other mature and unexplored Miocene strata of the northern Gulf of Mexico shelf province. Extrapolation of key sequence-stratigraphic surfaces that bound the third-order lowstand systems tracts from the fields throughout the 3-D seismic volume and into surrounding areas is an effective first step in defining the regional distribution of these proven hydrocarbon pools.

REFERENCES CITED

- Badescu, A. C., and H. L. Zeng, 2001, Integrating 3-D seismic, sequence stratigraphy, and reservoir properties to enhance secondary gas recovery of two major Miocene Gulf of Mexico offshore fields (abs.): AAPG Annual Meeting Program, v. 10, p. A10.
- Bebout, D. G., W. A. White, C. M. Garrett Jr., and T. F. Hentz, eds., 1992, Atlas of major central and eastern Gulf Coast gas reservoirs: University of Texas at Austin, Bureau of Economic Geology, 88 p.
- Berggren, W. A., D. V. Kent, and J. A. Van Couvering, 1985, Neogene chronology and chronostratigraphy, in N. J. Snelling, ed., The chronology of the geologic record: Geologic Society Memoir 10, p. 211–260.
- Berggren, W. A., D. V. Kent, C. C. Swisher III, and M.-P. Aubrey, 1995, A revised Cenozoic geochronology and chronostratigraphy, in W. A. Berggren, D. V. Kent, M.-P. Aubrey, and J. Hardenbol, eds., Geochronology, time scales and global stratigraphic correlation: SEPM Special Publication 54, p. 129–212.
- Boettcher, S. S., and K. L. Milliken, 1994, Mesozoic–Cenozoic unroofing of the southern Appalachian basin: apatite fission track evidence from Middle Pennsylvanian sandstones: Journal of Geology, v. 102, p. 655–663.
- Bowen, D. W., P. Weimer, and A. J. Scott, 1993, The relative success of siliciclastic sequence stratigraphic concepts in exploration: examples from incised valley fill and turbidite systems reservoirs, in P. Weimer and H. Posamentier, eds., Siliciclastic sequence stratigraphy: recent developments and applications: AAPG Memoir 58, p. 15–42.
- Crawford, T. G., B. J. Bascle, C. J. Kinler, M. T. Prendergast, and K. M. Ross, 2000, Outer continental shelf estimated oil and gas reserves, Gulf of Mexico, December 31, 1998: Minerals Management Service, U.S. Department of the Interior, OCS Report MMS 2000-069, 26 p.
- DeAngelo, M. V., and L. J. Wood, 2001, 3-D seismic detection of undrilled prospective areas in a mature province, South Marsh Island, Gulf of Mexico: Leading Edge, v. 20, p. 1282–1292.
- Diegel, F. A., J. F. Karlo, D. C. Schuster, R. C. Shoup, and P. R. Tauvers, 1995, Cenozoic structural evolution and tectono-stratigraphic framework of the northern Gulf Coast continental margin, in M. P. A. Jackson, D. G. Roberts, and S. Snelson, eds., Salt tectonics: a global perspective: AAPG Memoir 65, p. 109–151.
- Dutton, S. P., and T. F. Hentz, 2002, Reservoir quality of lower Miocene sandstones in lowstand prograding wedge successions, Vermilion Block 31, offshore Louisiana: Gulf Coast Association of Geological Societies Transactions, v. 52, p. 217–228.
- Erskine, R. D., and P. R. Vail, 1988, Seismic stratigraphy of the Exmouth Plateau, in A. W. Bally, ed., Atlas of seismic stratigraphy: AAPG Studies in Geology 27, v. 2, p. 163–173.
- Fillon, R. H., and P. N. Lawless, 1999, Paleocene–lower Miocene sequences in the northern Gulf: progradational slope salt-basin deposition and diminishing slope-bypass deposition in the deep basin: Gulf Coast Association of Geological Societies Transactions, v. 49, p. 224–241.
- Fillon, R. H., and P. N. Lawless, 2000, Lower Miocene–early Pliocene deposystems in the Gulf of Mexico: regional sequence relationships: Gulf Coast Association of Geological Societies Transactions, v. 50, p. 411–428.
- Galloway, W. E., 1989, Genetic stratigraphic sequences in basin analysis, II, application to northwest Gulf of Mexico basin: AAPG Bulletin, v. 73, p. 143–154.
- Galloway, W. E., L. A. Jirik, R. A. Morton, and J. R. DuBar, 1986, Lower Miocene (Fleming) depositional episode of the Texas coastal plain and continental shelf: structural framework, facies, and hydrocarbon resources: University of Texas at Austin, Bureau of Economic Geology Report of Investigations 150, 50 p.
- Galloway, W. E., P. E. Ganey-Curry, X. Li, and R. T. Buffler, 2000, Cenozoic depositional history of the Gulf of Mexico basin: AAPG Bulletin, v. 84, p. 1743–1774.
- Haq, B. U., J. Hardenbol, and P. R. Vail, 1988, Mesozoic and Cenozoic chronostratigraphy and cycles of sea-level change, in C. K. Wilgus, C. A. Ross, H. Posamentier, and C. G. St. C. Kendall, eds., Sea-level changes: an integrated approach: SEPM Special Publication 42, p. 71–108.
- Hardenbol, J., J. Thierry, M. B. Farley, T. Jacquin, P.-C. de Graciansky, and P. R. Vail, 1998, Mesozoic and Cenozoic sequence chronostratigraphic framework of European basins, in P.-C. de Graciansky, J. Hardenbol, T. Jacquin, and P. R. Vail, eds., Mesozoic and Cenozoic sequence stratigraphy of European basins: SEPM Special Publication 60, p. 3–13.
- Hart, G. F., R. E. Ferrell Jr., D. R. Lowe, and A. E. Lenoir, 1989, Shelf sandstones of the *Robulus* L zone, offshore Louisiana, in R. A. Morton and D. Nummedal, eds., Shelf sedimentation, shelf sequences and related hydrocarbon accumulation: Gulf Coast Section SEPM, 7th Annual Research Conference Proceedings, p. 117–141.
- Hentz, T. F., H. L. Zeng, and C. O. Kiliç, 2000, Sequence stratigraphy, depositional framework, and resource potential of mature gas reservoirs, Miocene of offshore Louisiana (abs.): AAPG Annual Meeting, CD-ROM.

- Hentz, T. F., H. L. Zeng, L. J. Wood, A. C. Badescu, C. Rassi, and C. O. Kiliç, 2001, Controls on hydrocarbon distribution within a sequence-stratigraphic framework: a case study from the Miocene of offshore Louisiana (abs.): AAPG Annual Meeting Program, v. 10, p. A86.
- Hentz, T. F., H. L. Zeng, and L. J. Wood, 2002, Sequence stratigraphy and hydrocarbon distribution of Miocene plays: a case study from Starfak and Tiger Shoal fields, offshore Louisiana (abs.): AAPG Annual Meeting Program, v. 11, p. A76–A77.
- Hunt, J. L., Jr., and G. Burgess, 1995, Depositional styles from Miocene through Pleistocene in the north-central Gulf of Mexico: an historical reconstruction: Gulf Coast Association of Geological Societies Transactions, v. 45, p. 275–284.
- Jiang, M. M., 1993, Miocene sequence biostratigraphy of the northern Gulf of Mexico: Gulf Coast Association of Geological Societies Transactions, v. 43, p. 137–143.
- Jiang, M. M., and J. S. Watkins, 1992, Floral pulses, foraminiferal peaks and inferred sequences in the Miocene of the northern Gulf of Mexico: Marine and Petroleum Geology, v. 9, p. 608–622.
- Lawless, P. N., R. H. Fillon, and R. G. Lytton III, 1997, Gulf of Mexico Cenozoic biostratigraphic, lithostratigraphic, and sequence stratigraphic event chronology: Gulf Coast Association of Geological Societies Transactions, v. 47, p. 271–282.
- Luo, X., 2000, 3D seismic interpretation of central offshore Louisiana, Gulf of Mexico: M.S. thesis, Baylor University, Waco, Texas, 72 p.
- McBride, E. F., L. S. Land, T. N. Diggs, and L. E. Mack, 1988, Petrography, stable isotope geochemistry and diagenesis of Miocene sandstones, Vermilion Block 31, offshore Louisiana: Gulf Coast Association of Geological Societies Transactions, v. 38, p. 513–523.
- McGookey, D. P., 1975, Gulf Coast Cenozoic sediments and structures: an excellent example of extra-continental sedimentation: Gulf Coast Association of Geological Societies Transactions, v. 25, p. 104–120.
- Minerals Management Service, 2001, The promise of deep gas in the Gulf of Mexico: Minerals Management Service, U.S. Department of the Interior, OCS Report MMS 2001-037, 4 p.
- Mitchum, R. M., and J. C. Van Wagoner, 1990, High-frequency sequences and eustatic cycles in the Gulf of Mexico basin, in J. M. Armentrout and B. F. Perkins, eds., Sequence stratigraphy as an exploration tool: concepts and practices in the Gulf Coast: Gulf Coast Section SEPM, 11th Annual Research Conference Proceedings, p. 257–267.
- Mitchum, R. M., J. B. Sangree, P. R. Vail, and W. W. Wornardt, 1990, Sequence stratigraphy in Late Cenozoic expanded sections, Gulf of Mexico, in J. M. Armentrout and B. F. Perkins, eds., Sequence stratigraphy as an exploration tool: concepts and practices in the Gulf Coast: Gulf Coast Section SEPM, 11th Annual Research Conference Proceedings, p. 237–256.
- Mitchum, R. M., J. B. Sangree, P. R. Vail, and W. W. Wornardt, 1993, Recognizing sequences and systems tracts from well logs, seismic data, and biostratigraphy: examples from the Late Cenozoic of the Gulf of Mexico, in P. Weimer and H. Posamentier, eds., Siliciclastic sequence stratigraphy: recent developments and applications: AAPG Memoir 58, p. 163–197.
- Morton, R. A., L. A. Jirik, and W. E. Galloway, 1988, Middle–upper Miocene depositional sequences of the Texas coastal plain and continental shelf: geologic framework, sedimentary facies, and hydrocarbon plays: University of Texas at Austin, Bureau of Economic Geology Report of Investigations 174, 40 p.
- Nehring, R., 1991, Oil and gas resources, in A. Salvador, ed., The Gulf of Mexico basin: Geological Society of America, Decade of North American geology, v. J, p. 445–494.
- Picou, E. B., Jr., B. F. Perkins, N. C. Rosen, and M. J. Nault, eds., 1999, Gulf of Mexico basin biostratigraphic index microfossils: a geoscientist's guide, foraminifers and nannofossils, Oligocene through Pleistocene: Gulf Coast Section SEPM Foundation, Parts I and II, 215 p.
- Posamentier, H. W., and P. R. Vail, 1988, Eustatic controls on clastic deposition, II, sequence and systems tract models, in C. K. Wilgus, C. A. Ross, H. Posamentier, and C. G. St. C. Kendall, eds., Sea-level changes: an integrated approach: SEPM Special Publication 42, p. 125–154.
- Rassi, C., 2002, Predicting reservoir performance through sequence stratigraphy—a viable approach? (abs.): AAPG Annual Convention, Official Program, v. 11, p. A145.
- Rassi, C., and T. F. Hentz, 2001, Production prediction and reservoir characterization of systems tracts of fourth-order sequences in the Miocene offshore Louisiana (abs.): AAPG Annual Meeting Program, v. 10, p. A164.
- Rosen, R. N., and W. A. Hill, 1990, Biostratigraphic application to Pliocene–Miocene sequence stratigraphy of the western and central Gulf of Mexico and its integration to lithostratigraphy: Gulf Coast Association of Geological Societies Transactions, v. 40, p. 737–743.
- Seni, S. J., T. F. Hentz, W. R. Kaiser, and E. G. Wermund Jr., eds., 1997, Atlas of northern Gulf of Mexico gas and oil reservoirs: volume 1. Miocene and older reservoirs: University of Texas at Austin, Bureau of Economic Geology, 199 p.
- Styzen, M. J., compiler, 1996, A chart in two sheets of the Late Cenozoic chronostratigraphy of the Gulf of Mexico: Gulf Coast Section SEPM Foundation.
- Van Wagoner, J. C., R. M. Mitchum, K. M. Campion, and V. D. Rahmanian, 1990, Siliciclastic sequence stratigraphy in well logs, cores, and outcrops: concepts for high-resolution correlation of time and facies: AAPG Methods in Exploration Series 7, 55 p.
- Wagner, J. B., B. M. Kofron, R. W. Morin, D. W. Ford, V. R. Mathur, and R. T. Mauro, 1994, A sequence stratigraphic analysis of the lower Miocene, West and East Cameron areas, Gulf of Mexico, in P. Weimer, A. H. Bouma, and B. F. Perkins, eds., Submarine fans and turbidite systems: sequence stratigraphy, reservoir architecture and production characteristics, Gulf of Mexico and international: Gulf Coast Section SEPM, 15th Annual Research Conference Proceedings, p. 357–372.
- Winker, C. D., 1982, Cenozoic shelf margins, northwestern Gulf of Mexico: Gulf Coast Association of Geological Societies Transactions, v. 32, p. 427–448.
- Zeng, H. L., 2001, From seismic stratigraphy to seismic sedimentology: a sensible transition: Gulf Coast Association of Geological Societies Transactions, v. 51, p. 413–420.
- Zeng, H. L., and L. J. Wood, 2002, Using quantitative seismic sedimentology to predict reservoir architecture and lithology: a Gulf Coast Miocene–Pliocene example (abs.): AAPG Annual Meeting Program, v. 11, p. A197.
- Zeng, H. L., T. F. Hentz, and L. J. Wood, 2000, Three-dimensional seismic facies imaging by stratal slicing of Miocene–Pleistocene sediments in the greater Vermilion Block 50-Tiger Shoal field area, offshore Louisiana (abs.): AAPG Annual Meeting Program, v. 9, p. A165.
- Zeng, H. L., T. F. Hentz, and L. J. Wood, 2001a, Stratal slicing of Miocene–Pliocene sediments in Vermilion Block 50-Tiger Shoal area, offshore Louisiana: Leading Edge, v. 20, p. 408–418.
- Zeng, H. L., T. F. Hentz, and L. J. Wood, 2001b, 3-D seismic expression of high-frequency sequence stratigraphy in Vermilion Block 50-Tiger Shoal area, offshore Louisiana (abs.): AAPG Annual Meeting Program, v. 10, p. A224–A225.
- Zeng, H. L., L. J. Wood, and T. F. Hentz, 2001c, Seismic sedimentology by stratal slicing of fluvial and shallow-marine depositional systems in Pliocene, offshore Louisiana: AAPG Annual Meeting Program, v. 10, p. A224.